COMPUTATIONAL MODELING OF ANTI-AGGREGATION EFFECT OF NON-STEROIDAL ANTI-INFLAMMATORY DRUGS IN ALZHEIMER'S AMYLOIDOGENESIS

by

Wenling E. Chang

A Dissertation
Submitted to the
Graduate Faculty
of
George Mason University
in Partial Fulfillment of
The Requirements for the Degree
of
Doctor of Philosophy
Bioinformatics and Computational Biology

Committee:

_____ Dr. Dmitri Klimov, Dissertation Director

_____ Dr. Saleet Jafri, Committee Member

_____ Dr. Iosif Vaisman, Committee Member

_____ Dr. Estela Blaisten-Barojas, Committee Member

_____ Dr. James Willett, Department Chairperson

_____ Dr. Richard Diecchio, Associate Dean for Academic and Student Affairs, College of Science

_____ Dr. Vikas Chandhoke, Dean, College of Science

Date: _____ Spring Semester 2011
George Mason University
Fairfax, VA

Computational Modeling of Anti-aggregation Effect of Non-steroidal Anti-inflammatory Drugs in Alzheimer's Amyloidogenesis

A dissertation submitted in partial fulfillment of the requirements for the degree of Doctor of Philosophy at George Mason University

By

Wenling E. Chang
Master of Science
Johns Hopkins University, 2004

Director: Dmitri Klimov, Associate Professor
Bioinformatics and Computation Biology

Spring Semester 2011
George Mason University
Manassas, VA

DEDICATION

This dissertation manuscript is dedicated to my loving, caring, and supportive parents.

ACKNOWLEDGEMENTS

I would like to thank Dr. Klimov, dissertation director, and my dissertation committee, Dr. Blaisten-Barojas, Dr. Jafri, and Dr. Vaisman for guiding me through the research process. I would like to thank my beloved parents, sisters, and Patrick for their support.

TABLE OF CONTENTS

LIST OF TABLES

LIST OF FIGURES

ABSTRACT

COMPUTATIONAL MODELING OF ANTI-AGGREGATION EFFECT OF NON-STEROIDAL ANTI-INFLAMMATORY DRUGS IN ALZHEIMER'S AMYLOIDOGENESIS

Wenling E. Chang, Ph.D.

George Mason University, 2011

Dissertation Director: Dr. Dmitri Klimov

Alzheimer's disease (AD) represents a growing biomedical, social, and economical problem. Millions of people have suffered from the disease globally. Studies have shown that aggregated forms of amyloid β peptide adversely affect neuronal function and may represent the causative agent in AD. It has been demonstrated that chronic treatment with ibuprofen and naproxen reduces the risk of AD and improves the behavioral impairment for patients with AD. This dissertation utilizes high performance parallel computing, all-atom molecular dynamics simulation, and protein-ligand docking to understand the mechanism of the anti-aggregation effect of ibuprofen and naproxen in Alzheimer's amyloidogenesis. The results reveal different mechanisms of ligand binding to the monomers and fibrils formed by Aβ peptides implicated in AD. Binding to Aβ monomers is mostly governed by ligand-amino acid interactions, whereas binding to the fibril is determined by the fibril surface geometry and interligand interactions. The anti-

aggregation effect of ibuprofen and naproxen is explained by direct competition between these ligands and incoming Aβ peptides for binding to the fibril.

1. INTRODUCTION

Alzheimer's disease (AD) progressively declines the cognitive function and introduces dementia. Studies have shown that the number of AD patients is projected to quadruple by 2050 [1]. Due to long term rehabilitation and costly medical treatments, AD imposes severe economical tolls on society. Currently the progression and the cause of AD are not well understood. A number of studies suggested that aggregated forms of Amyloid beta (Aβ or Abeta) peptides are the causative agents of AD.

Aβ is a peptide that is composed of 39 to 43 amino acids. It is formed due to proteolytic cleavage of the membrane bound amyloid precursor protein (APP). Aβ peptide is highly amyloidogenic and forms fibrils consisting of extensive cross β sheets that are stabilized by backbone hydrogen bonds (HBs) which are parallel to the fibril axis (**Figure 1**). The fibrils and other Aβ aggregates, such as oligomers, are neurotoxic and cause neuronal dysfunction and plasticity. However, the molecular mechanism underlying the neurotoxicity of Aβ remains speculative. It has been suggested that aggregated Aβ induces abnormalities in oxidative metabolism and specifically with the redox enzymes in mitochondria [2]. Aggregated Aβ elevates the formation of reactive oxygen species and free radicals. The peptide was also shown to promote apoptosis and induces the abnormalities of cellular calcium homeostasis [2]. Additionally, Aβ aggregates are known to disrupt the integrity of cellular lipid membranes and trigger the

formation of ion-permeable pores [3].

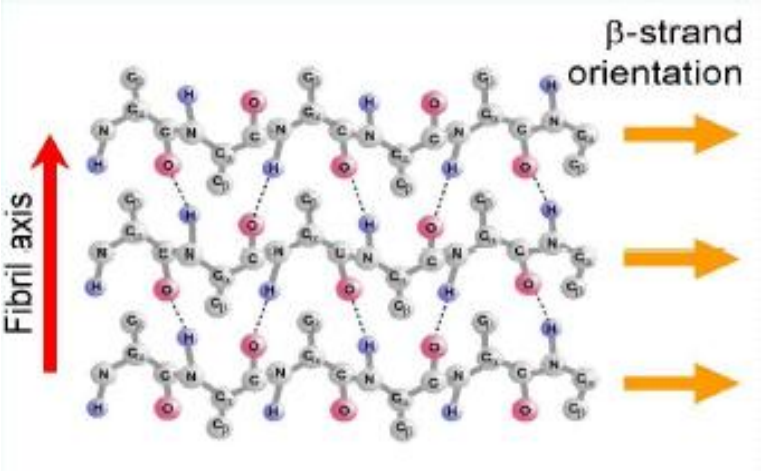

Figure 1 *The generic structure of amyloid fibril*

A promising strategy in AD treatment is to discover or design molecular anti-aggregation agents. Epidemiological findings have suggested that long-term treatment with non-steroidal anti-inflammatory drugs (NSAIDs) such as ibuprofen and naproxen significantly reduces the risk or delay the onset of AD [4, 5]. It has been speculated that NSAIDs elevate anti-inflammatory response against neurodegeneration caused by AD. Recent studies have also implied that NSAIDs can inhibit the formation and extension of β-amyloid fibrils (fAβ) formed from soluble Aβ as well as destabilize preformed fAβ [5]. A significant reduction in the formation and extension of fAβ was observed in vitro for fAβ(1-40) and fAβ(1-42) with the presence of NSAID. Interestingly, ibuprofen and

naproxen provided the strongest anti-aggregation effect among several NSAIDs tested [5].

To understand the anti-aggregation effect of ibuprofen and naproxen, it is necessary to first understand how these chemicals interact with Aβ peptides and fibrils as well as how Aβ peptide polymerizes into fibrils. Molecular docking can be utilized to determine the protein-ligand interaction by predicting the most favorable binding conformations between a ligand and a target protein. The calculated binding energies have been shown to be well correlated with experimental results and can be used to characterize protein binding pockets [6]. However, a disadvantage of molecular docking is that it has limited ability to model protein flexibility during substrate binding, potentially leading to incorrect sidechain and backbone conformations in the bound structure. This limitation may be specifically applicable to Aβ monomers and oligomers due to their highly mobile structure. It is highly recommended to use multiple docking tools to select the best protocol for interpreting the binding sites as predictions may vary based on the physical properties of protein structures [7]. Molecular dynamics (MD) can help overcome these potential inaccuracies by allowing the bound complex to reach thermodynamic equilibration.

To understand the aggregation and fibrillization of Aβ, Takeda and Klimov used molecular dynamics to determine the thermodynamics of fibril growth for $A\beta_{10-40}$ peptides, which are the truncated version of full-length $A\beta_{1-40}$ [8]. The simulations included the replica exchange molecular dynamics (REMD) and all-atom implicit solvent model [9]. The truncated peptides were evaluated instead of the full length ones to

increase the computational efficiency of the simulation and because the shortened peptides, $A\beta_{10-40}$, generally retain the structure of the full length peptides, $A\beta_{1-40}$ (see Methods). Therefore, one can expect that Takeda and Klimov's in silico model of the aggregation of Aβ peptides utilizing REMD simulations can be also applied to characterize these ligands' binding sites in Aβ fibrils and peptides.

The sequence for $A\beta_{10-40}$ peptides is defined as $Y_{10}EVHHQKLVFF_{20}$ $AEDVGSNKGA_{30}IIGLMVGGVV_{40.}$ In what follows residues 10 through 23 are referred as the N-terminal region (or β1), residues 24 through 28 are referred as the turn, and residues 29 through 39 compose the C-terminal region (or β2). The results presented in this dissertation were published in [10, 11, 12].

2. RESEARCH AIMS

This dissertation addresses the following three specific aims using the methods described in the Method section.

1. Use REMD to explore the binding of naproxen to Aβ fibril. The location of ligand binding sites in Aβ fibril as well as the mechanism governing naproxen binding will be determined. The results will be compared with the findings on fibril binding for ibuprofen reported in the previous publication by Klimov et al. [13]. Therefore, generality of fibril binding mechanisms independent on particular ligand can be established.
2. Use REMD to explore the impact of ibuprofen on fibril elongation. Aβ incoming peptides and fibril will be co-incubated with ibuprofen and the impact of the ligand on peptide deposition onto the fibril will be evaluated by comparing with the findings on fibril growth in the absence of the ligand reported by Klimov et al. earlier [13]. Aggregation free energy landscape affected by ibuprofen will be analyzed. In particular, it is important to determine if ibuprofen reduces the free energy gain obtained by incoming Aβ peptide upon its deposition. Therefore, the molecular mechanisms of ibuprofen anti-aggregation effect will be determined.
3. Compare REMD simulation findings with available experimental observations.

3. METHODS

Recent solid-state NMR studies have shown that the fibril structures of Aβ(1-40) and Aβ(10-40) are remarkably similar and the first nine residues at the N-terminal of Aβ1−40 are structurally disordered [14, 15, 16, 17]. Takeda and Klimov's recent molecular dynamics (MD) simulations suggested that the conformational ensembles of Aβ(1-40) and Aβ(10-40) monomers and dimers are also very similar [8]. Consequently, Aβ(10-40) peptide is used as a model for the full-length wild-type peptide.

3.1. DESCRIPTION OF FORCE FIELD

CHARMM molecular dynamics (MD) program [18] and united atom force field CHARMM19 coupled with the SASA implicit solvent model [19] were used in the simulations. It has been previously shown that CHARMM19+SASA force field accurately reproduces the experimental distribution of chemical shifts for Cα and Cβ atoms in Aβ monomers [20, 21]. The force field description for ibuprofen and naproxen can be found below.

3.1.1 FORCE FIELD PARAMETERS FOR IBUPROFEN

The standard release of CHARMM force field does not offer parameterization for ibuprofen. To parameterize ibuprofen, existing CHARMM19 atom types were used. The charges were assigned consistently with the standard charges in the CHARMM19 force field and SASA implicit solvent model. The dihedral and improper angle potentials were

transferred from structurally analogous amino acids Phe, Glu, Trp, and Asp. The following specific modifications were made in topology top19_eef1.inp file:

```
RESI IBU    0.00000
! IBUPROFEN
! C16                    C6 - C5                  O10
!     > C14 - C13 - C1 <         > C4 - C7 - C8 <
! C15                    C2 - C3        |         O9
!                                       C9
GROUP
ATOM C1   CR      0.00
ATOM C2   CR1E    0.00
ATOM C3   CR1E    0.00
ATOM C4   CR      0.00
ATOM C5   CR1E    0.00
ATOM C6   CR1E    0.00
GROUP
ATOM C13  CH2E    0.00
ATOM C14  CH1E    0.00
ATOM C15  CH3E    0.00
ATOM C16  CH3E    0.00
GROUP
ATOM C7   CH1E   -0.15
ATOM C8   C       1.35
ATOM C9   CH3E    0.00
ATOM O9   OC     -0.60
ATOM O10  OC     -0.60
BOND C14  C15    C14  C16       C13  C14       C1   C13       C1   C2
```

The following parameters for bond, dihedral, and improper angles were added to the parameter param19_eef1.inp file:

```
!...bond angles...
CR1E CR   CH1E    70.0     121.5
CR   CH1E C       70.0     112.5
```

```
CR   CH1E CH3E    70.0     106.5

!...dihedral angles
CR1E CR   CH1E C        0.0       3       0.0

!...improper angles…
CR   CR1E CR1E CH1E    90.0    0     0.0
CH1E C    CH3E CR      55.0    0   35.26439
```

The ibuprofen force-field parameters were further verified. The in silico distribution of internal dihedral angles in ibuprofen was found consistent with the density functional theory calculations and vibrational spectroscopy [13].

3.1.2 FORCE FIELD PARAMETERS FOR NAPROXEN

To parameterize naproxen existing CHARMM19 atom types were also used. The charges were assigned in a manner consistent with the standard charges in the CHARMM19 force field and SASA implicit solvent model. Charges in the methoxy group were assigned using the parameterization of trimethoprim molecule [22]. The bond length and bond angle terms were automatically determined. The dihedral and improper angle potentials were derived from structurally analogous amino acids Phe, Glu, Trp, and Asp. An additional improper angle for C14 atom was introduced as in branched side chain of Ile. The modifications were made in the topology top19_eef1.inp file as shown below.

```
RESI NPXN 0.00000
! naproxen
!          C7  C12    C14
!         // \ / \\    |
!        C8  C6   C11-C13-C15--O16
!        |   ||   |       |
!        C3  C5   C10     O17
!       / \\ / \ //
! C1--O2  C4  C9
```

```
GROUP
ATOM  C1    CH3E  0.15
ATOM  O2    OS    -0.3
ATOM  C3    CR    0.15
GROUP
ATOM  C4    CR1E  0
ATOM  C5    CR    0
ATOM  C6    CR    0
ATOM  C7    CR1E  0
ATOM  C8    CR1E  0
ATOM  C9    CR1E  0
ATOM  C10   CR1E  0
ATOM  C11   CR    0
ATOM  C12   CR1E  0
GROUP
ATOM  C13   CH1E  -0.15
ATOM  C14   CH3E  0
ATOM  C15   C     1.35
ATOM  O16   OC    -0.6
ATOM  O17   OC    -0.6
BOND  C1    O2    O2    C3    C3    C4    C4    C5    C5    C6
BOND  C6    C7    C7    C8    C8    C3    C5    C9    C9    C10
BOND  C10   C11   C11   C12   C12   C6    C11   C13   C13   C14
BOND  C13   C15   C15   O16   C15   O17
DIHE  C4    C3    O2    C1
DIHE  C11   C13   C15   O17   C12   C11   C13   C15
DIHE  C4    C5    C6    C12   C7    C6    C5    C9
DIHE  C8    C6    C5    C10   C8    C5    C6    C11
IMPH  C3    C4    C8    O2    C13   C15   C14   C11
IMPH  C15   O16   O17   C13   C11   C10   C12   C13
IMPH  C3    C4    C5    C6    C4    C5    C6    C7    C5    C6    C7
      C8
IMPH  C6    C7    C8    C3    C7    C8    C3    C4    C8    C3    C4
      C5
IMPH  C5    C9    C10   C11   C9    C10   C11   C12   C10   C11   C12
      C6
IMPH  C11   C12   C6    C5    C12   C6    C5    C9    C6    C5    C9
      C10
IC    C1    O2    C3    C4    0     0     180   0     0
```

```
IC    O2    C4    *C3   C8    0     0     180   0     0
IC    C3    C4    C5    C6    0     0     0     0     0
IC    C4    C5    C6    C7    0     0     0     0     0
IC    C5    C6    C7    C8    0     0     0     0     0
IC    C10   C9    C5    C6    0     0     0     0     0
IC    C9    C5    C6    C12   0     0     0     0     0
IC    C5    C6    C12   C11   0     0     0     0     0
IC    C6    C4    *C5   C9    0     0     180   0     0
IC    C5    C7    *C6   C12   0     0     180   0     0
IC    C10   C12   *C11  C13   0     0     180   0     0
IC    C12   C11   C13   C15   0     0     0     0     0
IC    C11   C15   *C13  C14   0     0     -120  0     0
IC    C11   C13   C15   O16   0     0     0     0     0
IC    C13   O16   *C15  O17   0     0     120   0     0
```

The following parameters for bond, dihedral and improper angle potentials were added.

```
!...bond angles...
CR1E  CR    CH1E  70    121.5
CR    CH1E  C     70    112.5
CR    CH1E  CH3E  70    106.5
CR    CR1E  CR    90    119
CR    OS    CH3E  46.5  120.5
CR1E  CR    OS    65    119

!...dihedral angles
CR1E  CR    CH1E  C     1.6   3     0
CR1E  CR    OS    CH3E  1.8   2     180

!...improper angles…
CR    CR1E  CR1E  CH1E  90    0     0
CH1E  C     CH3E  CR    55    0     35.26439

CR    CR1E  CR1E  OS    150   0     0
```

The solvation parameters for ester OS atom were set to be the same as the hydroxyl oxygen. The parameterization in CHARMM19 was tested by building the naproxen molecule in all-atom CHARMM general force field Cgenff. The energy-

minimized structures in both force fields were very similar.

3.2 SIMULATION SYSTEMS

Three simulation systems were utilized and described in Sections 3.2.1, 3.2.2, and 3.2.3.

3.2.1 SIMULATION SYSTEM FOR NAPROXEN WITH ABETA FIBRIL

Forty naproxen molecules were placed randomly in the vicinity of $A\beta_{10-40}$ peptides resulting in a ratio of Aβ and naproxen concentrations of 1:10 (**Figure 2a**). The Aβ system with naproxen is subject to a spherical boundary condition with the radius R_s=90 Å and the force constant k_s=10 kcal/(molÅ^2).The fibril structure was modeled using the coordinates of backbone atoms derived from the solid-state NMR measurements [23]. The backbones of fibril peptides (**Figure 2a**) were constrained to their experimental positions using soft harmonic potentials with the constant k_c=0.6 kcal/(molÅ^2) [9]. The harmonic constraints permit backbone fluctuations with the amplitude of about 0.6Å at 360 K, which are comparable to the fluctuations of atoms on the surface of folded proteins [24]. The harmonic constraints emulate the stability of amyloid fibril, which is known to be highly resistant to dissociation [25] and eliminate the necessity to simulate large fibril systems to achieve their stability. This simulation system is referred to as System 1.

3.2.2 SIMULATION SYSTEM FOR Aβ FIBRIL AND TWO INCOMING PEPTIDES COINCUBATED WITH IBUPROFEN

The fibril structure (in grey, **Figure 2b**) is modeled using the coordinates of backbone atoms determined from the solid-state NMR measurements [15] and consists of

four peptides. This fibril fragment is identical to that used in System 1. In addition to the fibril, this simulation system includes two incoming peptides and 60 ibuprofen molecules (**Figure 2b**). The harmonic constraints (as in System 1) were not applied to the side chains of fibril peptides or to the incoming peptides, which were free to associate or dissociate from the fibril. Similar to System 1 spherical boundary conditions were applied. In what follows this simulation system is referred to as System 2. Note that in both systems the ratio of the numbers of ligands and peptides is 10:1, which is within the range used experimentally (from 1 to 22) [11].

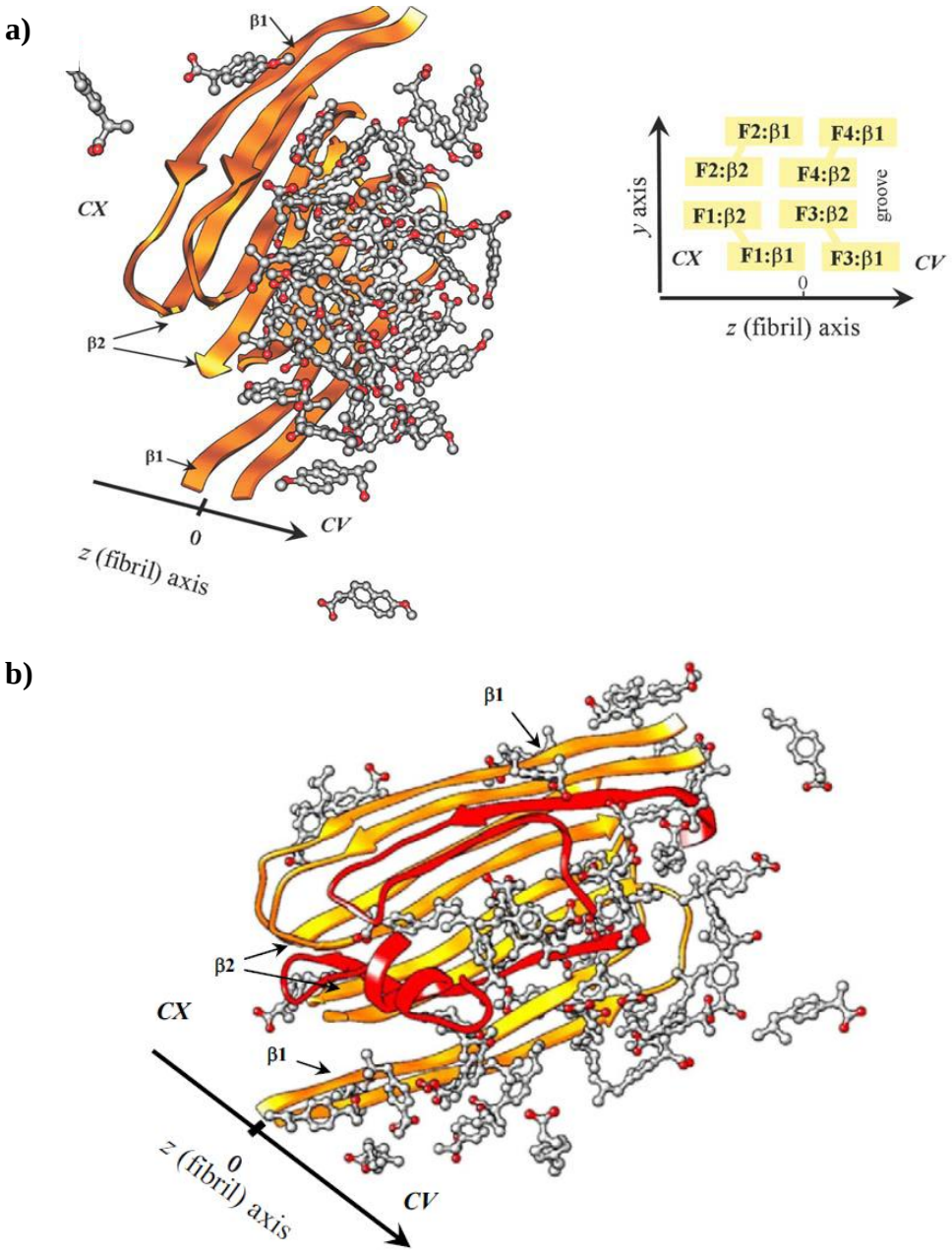

Figure 2 *(a) Simulation system 1: The snapshot of naproxen molecules placed in the vicinity of Aβ fibril, which consists of the peptides F1, F2, F3 and F4 as shown in the diagram. The structure of Aβ10-40 fibril derived from solid-state NMR measurements. This simulation system was used to study binding of naproxen to Aβ fibril. The indented β2 sheets form a groove which creates two distinct edges: CV (concave) and CX (convex). The CX and CV edges are respectively comprised of the F1, F2 and F3, F4 peptides. The groove on the CV edge is the primary binding site for naproxen and ibuprofen. (b) Simulation system 2: Two incoming peptides in color are bound to the*

fibril tetramer fragment. Together with 60 ibuprofen molecules, this system was designed to investigate the anti-aggregation effect of the NSAID ligands.

3.3 REPLICA EXCHANGE SIMULATIONS

Replica exchange molecular dynamics (REMD) is utilized to achieve exhaustive conformational sampling [26]. This method has exhibited high efficiency in sampling rugged free energy landscapes and has been applied to study protein folding and aggregation [9, 27, 28, 29, 30, 31, 32]. A total of 24 replicas were distributed linearly in the temperature ranges from 330 to 560 K for Systems 1 and 2 with an increment of 10K. The exchanges were attempted every 20ps between all neighboring replicas. Based on the previous results, four (System 1) and fourteen (System 2) independent REMD trajectories were produced to achieve the convergence of conformational sampling [9, 27]. The cumulative simulation times were 14.4 μs and 67 μs for Systems 1 and 2, respectively. Between each of the replica exchanges, the systems were evolved using NVT under-damped Langevin dynamics with the damping coefficient of γ=0.15 ps^{-1} and the integration step of 2 fs. To determine the REMD equilibration interval τ_{eq}, the effective energy E_{eff}, which includes the potential and solvation energies, was monitored. As a result, the initial parts of REMD trajectories corresponding to equilibration were excluded. The cumulative equilibrium simulation times were reduced to 13 μs and 56 μs for Systems 1 and 2, respectively. The REMD trajectories were started with random distribution of ligands in the sphere and random conformations of incoming Aβ peptides.

3.4 COMPUTATION OF STRUCTURAL PROBES

To compute ligand-peptide interactions the following structural groups were defined in the ligands. In ibuprofen, two hydrophobic groups, C1-C6 (G1) and C12-C15 (G2), and one hydrophilic group, C7-C9, O10, O11 (G3), were distinguished (**Figure 3**). For naproxen, there are one hydrophobic group, C3-C12 (G1), and two hydrophilic groups, C1-O2 (G2) and C13-O17 (G3) (**Figure 3**).

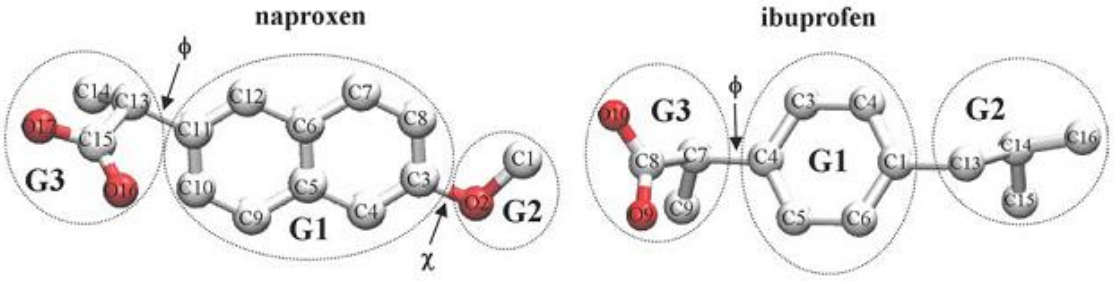

Figure 3 *The structures of ibuprofen and naproxen. Naproxen molecule has a central hydrophobic naphthalene ring (group G1), methoxy (G2), and carboxylate groups (G3). Ibuprofen has three structural moieties: hydrophobic phenyl (G1) and isobutyl (G2), and hydrophilic carboxylate (G3). Carbon is grey, and oxygen is red.*

A ligand is considered to be in contact with a side-chain, if the center of mass of one of the groups (G1, G2, or G3) is less than 6.5 Å from the side-chain center of mass. Also, if the center of mass of a side-chain is less than 6.5 Å from another side-chain center of mass, then a side-chain to side-chain contact is formed. The occurrences of HBs between ligand and peptide and between peptides were monitored by the methods of

Kabsch and Sander [33]. The HBs were classified into three different types: peptide-fibril HBs, parallel peptide-fibril HBs (pHBs), and antiparallel peptide-fibril HBs (aHBs). The pHBs are involved in the formation of parallel β-sheets on the fibril edge, whereas the aHBs are involved in the formation of anti-parallel β-sheets. The accessible surface areas (ASAs) were computed using Lee and Richards' algorithm [34]. The multiple histogram method was used to analyze the distributions of states produced by REMD and to compute thermodynamic quantities [35]. The angular brackets <..> imply thermodynamic averages.

3.5 PROTEIN-LIGAND DOCKING SIMULATIONS

Protein-ligand docking simulations were performed for naproxen. To obtain the ensemble of $A\beta_{10-40}$ monomer structures coincubated with the ligand at 330K, the REMD simulation data generated in the previous studies of Klimov et al [36] was used. In all, a total of 640 Aβ snapshots were considered. Using this REMD-generated conformational ensemble the ligand binding to diverse Aβ structures can be studied.

For the AutoDock simulations, atom types and partial charges were calculated for Aβ and ligand using the prepare_receptor4.py and prepare_ligand4.py scripts in the AutoDockTools toolkit [37]. The gridcenter was set to be auto. A grid resolution of 0.375Å was used with 40 points in the x, y, and z directions. AutoDock was run using the Lamarckian Genetic Algorithm (LGA) and semiempirical energy function. To verify the LGA results, Simulated Annealing (SA) was also utilized as the search algorithm. The protein was kept rigid during the docking process whereas the ligand was treated as flexible.

For the LGA simulation, the initial population size was set to 150, and the maximum number of energy calculations was set to 2.5×10^7. The default options were used for the pseudo-Solis and Wets local searches. For each simulation, ten independent iterations of the LGA were performed and clustering was utilized with a RMS tolerance of 2.0Å. For the SA simulation, the initial annealing temperature was set to 337K. The annealing temperature reduction per cycle was set to 0.99. The maximum steps accepted and rejected were at 30,000.

For each of the 640 snapshots, 10 ligand conformers with the lowest energy were predicted. Any residue that has at least one atom (including hydrogen) within 6.5 Å of any ligand atom is identified as a in contact with the ligand. The probability for each Aβ residue to be in contact with the ligand was determined by dividing the total number of contacts for each residue by the number of conformations examined (6,400).

4. INTERACTION OF NAPROXEN WITH Aβ FIBRIL

4.1 RESULTS

4.1.1 BINDING OF NAPROXEN TO AB FIBRILS

The probabilities of binding of naproxen to the fibril as a function of temperature were determined using System 1. As shown in **Figure 4**, the binding midpoint occurs around 398 K. At 360 K, the probability of binding (P_b) for naproxen to the fibril is 0.72 and the number of bound ligands is 28.8. In comparison, P_b for ibuprofen is 0.63 at 360K. This observation indicates a higher binding affinity of naproxen than of ibuprofen for binding to Aβ fibril. The free energy of naproxen binding to the fibril was studied as a function of the distance r_b between the ligand and the fibril surface at 360 K. In **Figure 5**, the free energy of binding ΔF_b was calculated according to:

$$\Delta F_b = F_b - F_a \quad (1)$$

$$F_b \leq F_{min} + 1.0\ RT$$

where F_b and F_a=0 are the free energies of bound and unbound states and F_{min} is free energy at the minimum. The result shows that $\Delta F_b \approx$ -7.6 RT for the binding of naproxen to the fibril. Because for ibuprofen ΔF_b = -5.2RT, the naproxen bound state is more stable than of ibuprofen by $\Delta\Delta F_b = \Delta F_b$ (npxn)- ΔF_b (ibu) = -2.0 RT.

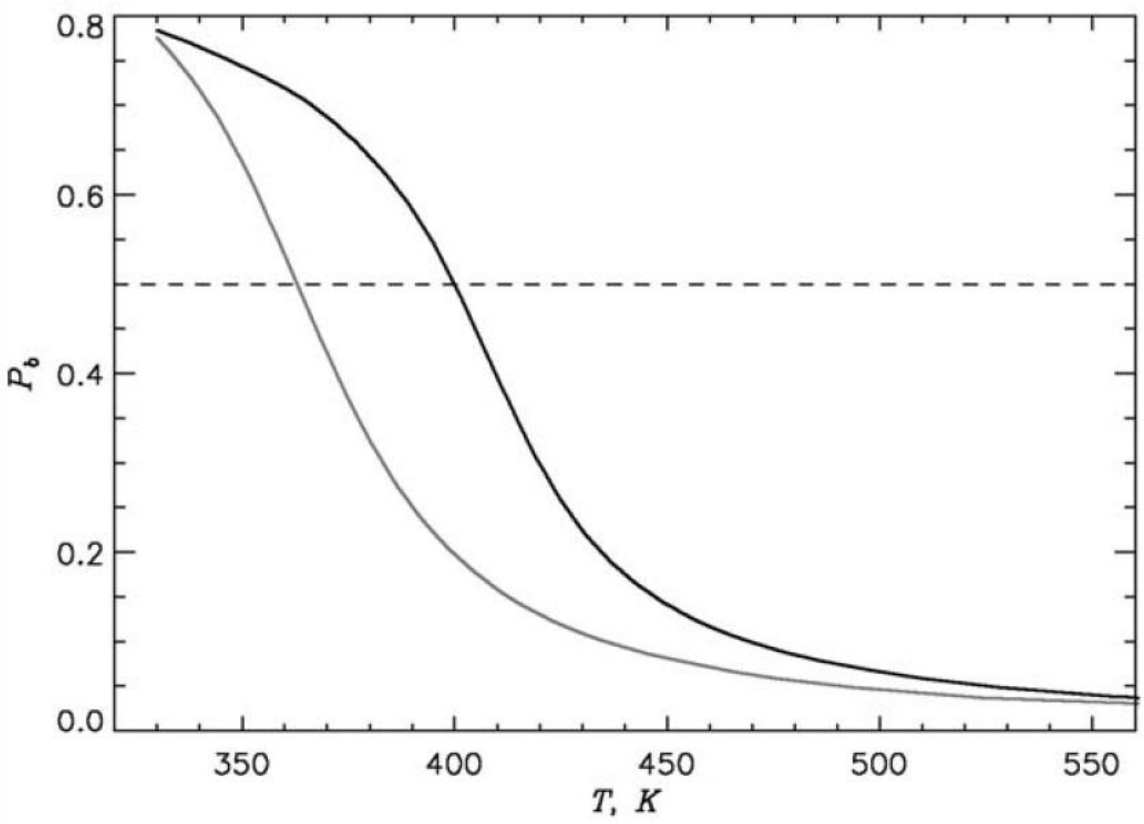

Figure 4 *The probability of naproxen (black line) or ibuprofen (grey line) binding to Aβ fibril as a function of temperature.*

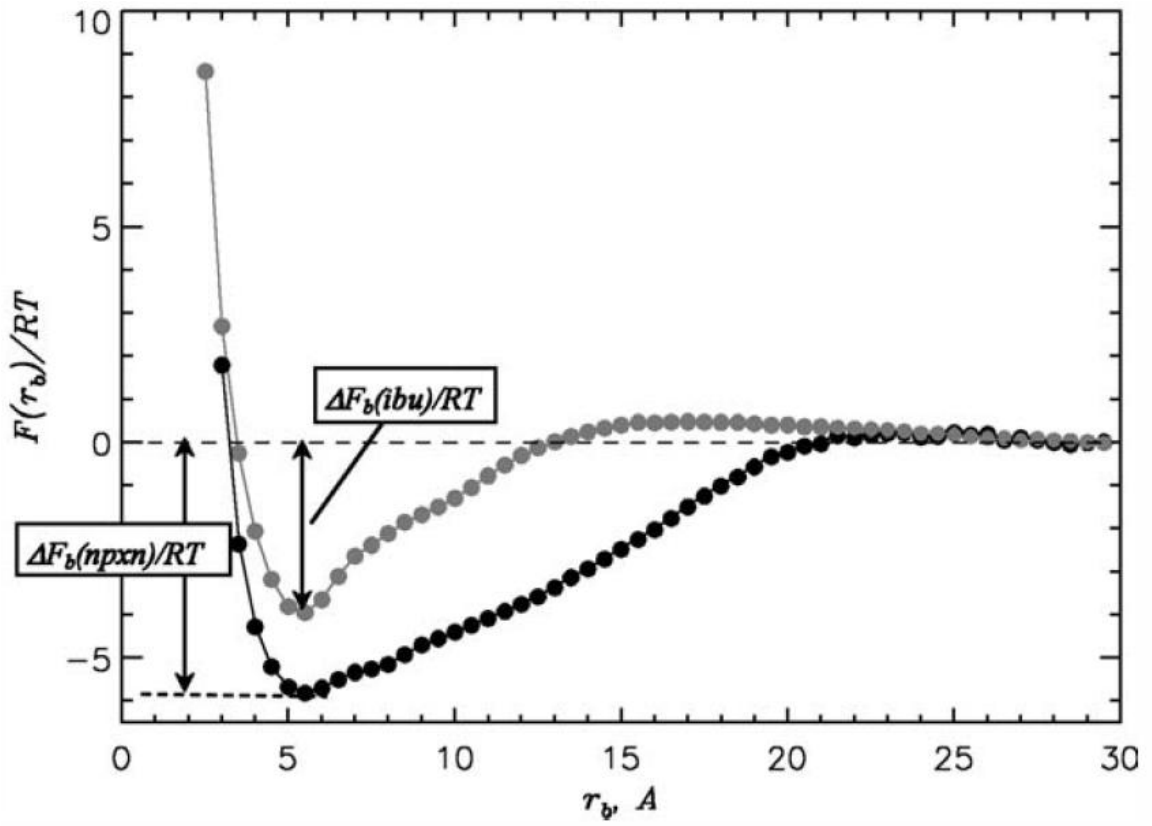

Figure 5 *Free energy profile for naproxen (in black) or ibuprofen (in grey) to bind to Aβ fibril as a function of the distance between the ligand and the Aβ fibril surface at 360 K. All values of F at r_b greater than 30 Å are set to zero.*

It is possible that the structure of the Aβ fibril plays a role in binding affinities. The Aβ structure contains two distinct edges [15]. They are the concave (CV) edge with the groove and the convex (CX) edge with the protrusion (**Figure 2a**). **Figure 6** displays the number of naproxen molecules bound to the CV and CX edges, $<L_{CV}(T)>$ and $<L_{CX}(T)>$ as a function of temperature. At temperatures less than 390 K, $<L_{CV}(T)>$ continues increasing as temperature decreases, while $<L_{CX}(T)>$ begins to decrease. At

360K, $<L_{CV}(T)>$ is double that of $<L_{CX}(T)>$. Similar behavior is observed for ibuprofen but at lower temperatures. Hence structure does appear to affect the binding affinity of the ligands in a significant manner. The binding affinity is stronger for the CV edge rather than for the CX.

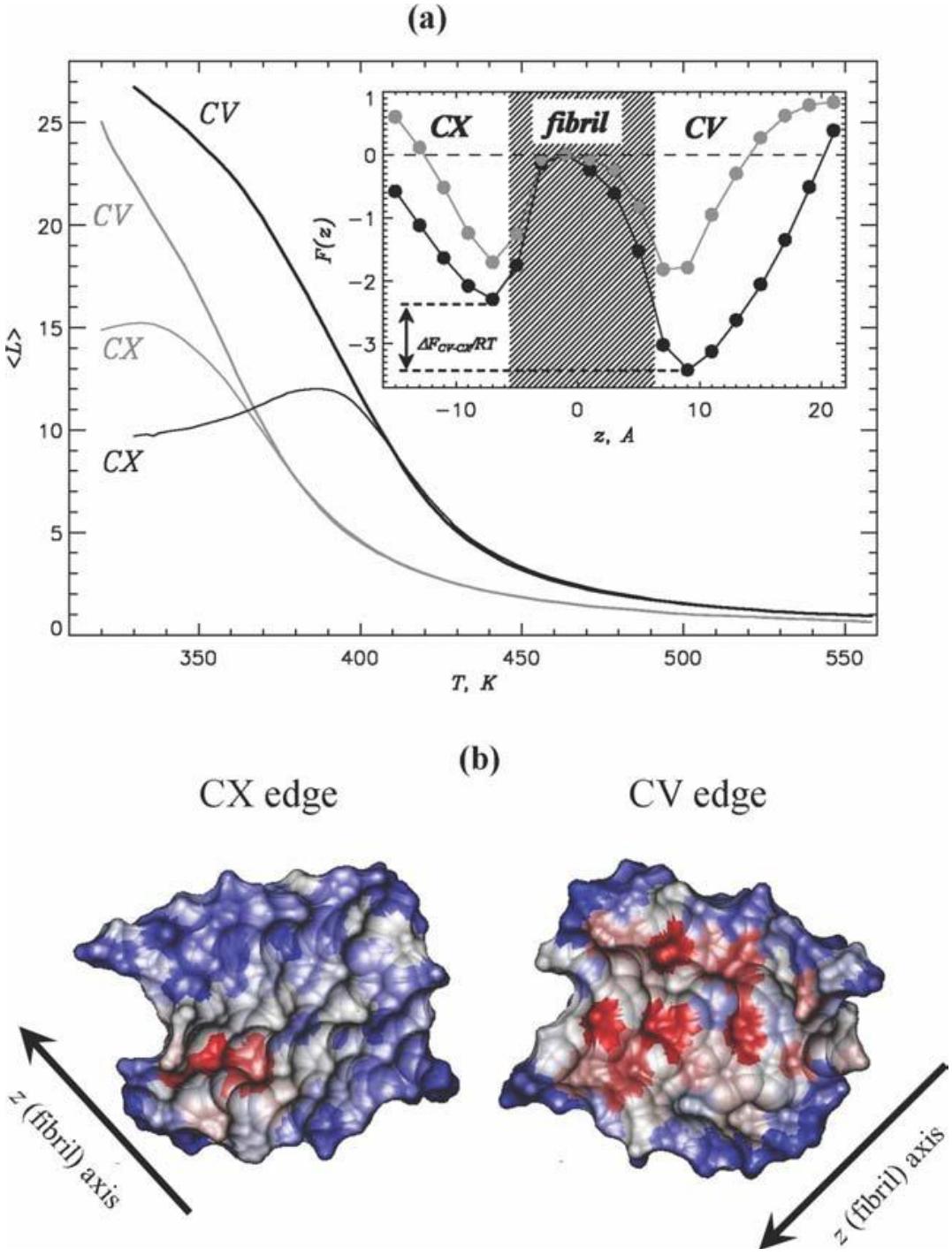

Figure 6 *(a) <L> is the numbers of ligand molecules bound to the CV (thick lines) and CX (thin lines) edges. Naproxen data is in black and ibuprofen [13] - in grey (including the inset). Inset: The free energy of a ligand F(z) along the fibril axis z (**Figure 2a**) at 360 K. The shaded area approximates the fibril's extent. (b) CV and CX fibril edge*

surfaces accessible to naproxen upon binding at 360 K. Red, grey, and blue correspond to large, medium, and small numbers of side chain contacts with naproxen, respectively.

The formation of ligand-amino acids contacts and hydrogen binds (HB) (see Methods) were analyzed. There are, on an average, 69.3 contacts with the CV edge ($<C_{CV}>\approx 69.3$) and an average of 31.5 contacts with the CX edge ($<C_{CX}>\approx 31.5$). However, there are only an average of 5.9 HBs formed between naproxen and the fibril's CV edge and 4.1 HBs formed between naproxen and the fibril's CX edge. Therefore, naproxen has more than 10 times as many contacts with the fibril side chains than it forms HBs with the fibril backbone. In comparison, at 360 K, ibuprofen has 41.4 and 37.1 contacts with the fibril CV and CX edges, respectively [13]. In that case, the corresponding numbers of HBs are 2.8 and 4.3, so ibuprofen's ratio of side chains to HBs is also close to 10. Thus, both ligands bind to the fibril largely by using interactions with the peptide side chains rather than backbone HBs.

The ligand free energy F(z) along the fibril axis z (**Figure 2a**) provides further evidence that the edges binding affinities are different. Naproxen and ibuprofen two have minima in free energy: one due to binding to the CV edge, and one due to binding to the CX (**Inset to Figure 6**). However, the naproxen free energy minima differ noticeably in magnitude. The free energy gap between CV and CX bound states, $\Delta F_{CV\text{-}CX}$, is about -1.1 RT for naproxen, but close to 0 for ibuprofen. Furthermore, the probabilities of binding to the edges were estimated by assuming that ligand is bound to CX or CV edges, if its z-

value is between -15 Å and -3 Å or between 3Å and 17 Å, respectively (**Figure 6a**). For naproxen, the probability of ligand occurrence on the CX edge was 0.69, and on the CV edge it was 0.21, whereas for ibuprofen the difference is smaller (on the CX edge with the probability of 0.26 and on the CV edge with the probability of 0.37). Only at 330 K does ibuprofen displays a preference for the CV edge, occurring there with the probability 0.57 as opposed to 0.29 on the CX edge [13]. The probability for finding either naproxen or ibuprofen on the fibril side (-3<z<3) was very small (0.01 and 0.04 respectively).

It is useful to determine how naproxen is distributed on the surface of Aβ fibril. **Figure 6b** displays the distribution of naproxen which is colored based on the number of contacts each amino acid forms with the ligands. The amino acids which have large number of contacts are located in the CV groove. To identify the amino acids, which constitute the naproxen binding sites, the following procedure [13] was used. An amino acid i is considered a part of the CV binding site, if the number of contacts with naproxen, $<C_l(i;k)>$, is no less than 70% of the maximum value on the CV edge, ($<C_l(i;k)> \geq 0.7\ \max_{i,k}\{<C_l(i;k)>\}$), where k=F3,F4 (**Figure 2a**). The naproxen binding site on the CV edge was found to include Gln15(F3), Gly29(F3), Ile31(F3), Leu34(F3), Met35(F3), Gly37(F3), Val39(F3), Glu11(F4), Gln15(F4), Leu17(F4), Phe19(F4), and Asp23(F4). The same procedure applied to the CX edge identified Asp23(F1), Ser26(F1), Ala30(F1), and Ile32(F1) as part of the CX binding site. Out of 16 amino acids involved in binding, half are hydrophobic and 11 are also implicated in ibuprofen binding at 330K [13]. In other words, hydrophobic and hydrophilic residues equally

contribute to naproxen binding and the majority of these residues are also implicated in the case of ibuprofen.

To get additional insight on the difference in binding affinities of naproxen and ibuprofen, the number of ligand-fibril contacts per ligand molecule at 360 K was considered. There are an average of 3.1 and 3.0 contacts between a naproxen and the fibril's CV and CX edges, respectively. Ibuprofen has an average of 3.1 contacts on both edges. Since these numbers are nearly the same, the differences in binding affinities between the ligands cannot be explained by ligand-fibril interactions (See Discussion). Thus, it appears that naproxen (and ibuprofen) binding is driven mainly by fibril surface geometry rather than by specific physicochemical properties of the residues (see below).

4.1.2 FIBRIL SURFACE GEOMETRY DETERMINES BINDING

The results of REMD computations of naproxen binding suggest a highly uneven distribution of ligands on the fibril surface. Most of the molecules are localized on the CV edge, whereas the CX edge and the fibril sides have significantly lower affinity. **Figure 7a** shows the probability distributions, P(y), of naproxen molecules along the y axis perpendicular to the fibril axis (**Figure 2a**). The probability, $P_{CV}(y)$, on the CV edge shows a pronounced maximum. However, the probability, $P_{CX}(y)$ on the CX edge is low. More importantly, the maximum in $P_{CV}(y)$ coincides exactly with the location of the groove, and the minimum of $P_{CX}(y)$ coincides with the location of the protrusion. As was the case with ibuprofen [13], these data indicate that naproxen tends to localize in the deep indentations on the fibril surface.

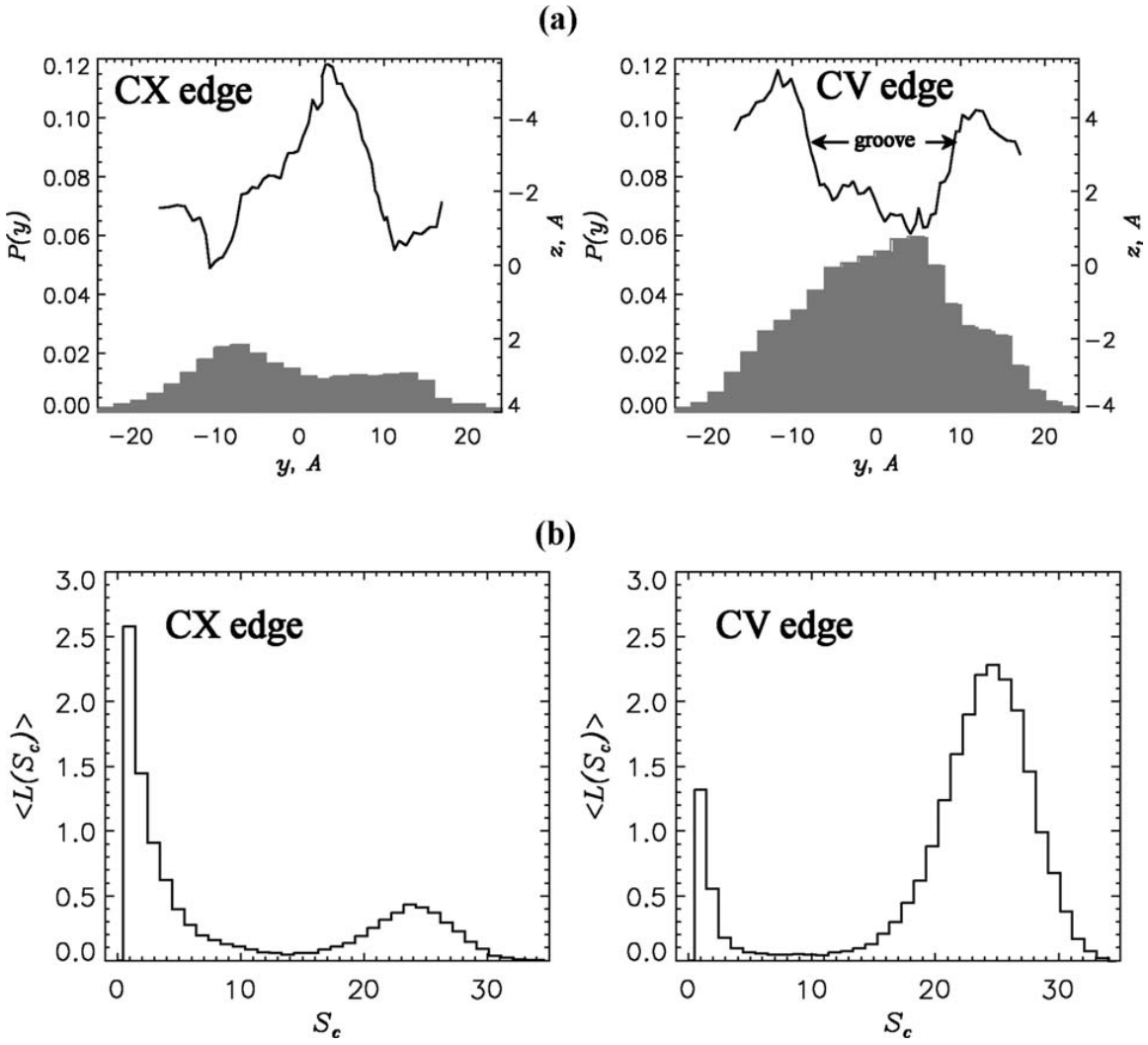

Figure 7 *(a) Probabilities of occurrence of naproxen molecule center of mass, P(y) (in grey), along the axis y perpendicular to the fibril axis z. The left and right panels are computed for z < 0 (CX edge) and z > 0 (CV edge), respectively (**Figure 2b**). Smoothed projections of the edge surfaces on the (y,z) plane are in black. The edge surface is represented by the side chain centers of mass. (b) Distributions of the numbers of bound ligands <L(Sc)> with respect to cluster size Sc. All results were computed at 360 K.*

To establish the factors which enhance the affinity of the CV edge, clusters formed by bound naproxen ligands on the fibril edges were examined. A cluster is a set of ligands bound to the fibril edge, which does not contact any other bound molecules. The size of a cluster S_c is equal to the number of included ligands. Then binding to a fibril edge can be characterized by the distribution of bound ligands over clusters, $<L(S_c)>$, where $<L>$ is the thermally averaged number of molecules in the clusters of size S_c. **Figure 7b** shows that the distribution, $<L(S_c)>$, for the CV edge has two peaks at S_c=1 and 25. Clusters with a size greater than 6 ($S_c > 6$) are considered to be large. The percentage of large clusters found on the CV and CX edges are denoted φ_{CV} and $\varphi_{CX,}$ respectively. The number of naproxen molecules forming large clusters, $<L_{CV,l}>$, is approximately 20.2 out of $<L_{CV}>\approx 22.5$, the total the number of ligands bound to the CV edge, i.e. φ_{CV}=0.90. In striking contrast, on the CX edge, $<L_{CX,l}>$, is found to be approximately 4.4, which constitutes 42% of $<L_{CX}>\approx 10.6$, i.e., φ_{Cx}=0.42. Therefore, about 90% of naproxen molecules bound to the CV form large clusters. In contrast, most (58%) of the ligands bound to the CX edge form small or no clusters. At 360 K, the distribution of ibuprofen clusters on both edges is unimodal and qualitatively different from that computed for naproxen. For example, the fractions of ligands forming large clusters are φ_{CV}=0.43 and φ_{CX} = 0.25. Only at 330K, do the distributions for bound ibuprofen become bimodal with φ_{CV}=0.81 and φ_{CX}=0.40 and resemble those for naproxen [13].

Figure 8 substantiates the conjecture that ligand-ligand interactions are important factor in binding, as suggested by the formation of large clusters on the CV edge. The

radial distribution function for naproxen number density, g(r), measures the local number density of ligands at the distance r from a given ligand. For naproxen, g(r) peaks at 4.5 Å, and is four or three times the bulk value g_0, for the CV or CX edges, respectively. In contrast, g(r) for ibuprofen has a maximum at 5.5 Å, which is only 1.5 times larger than g_0, and is the same for the CV and CX edges.

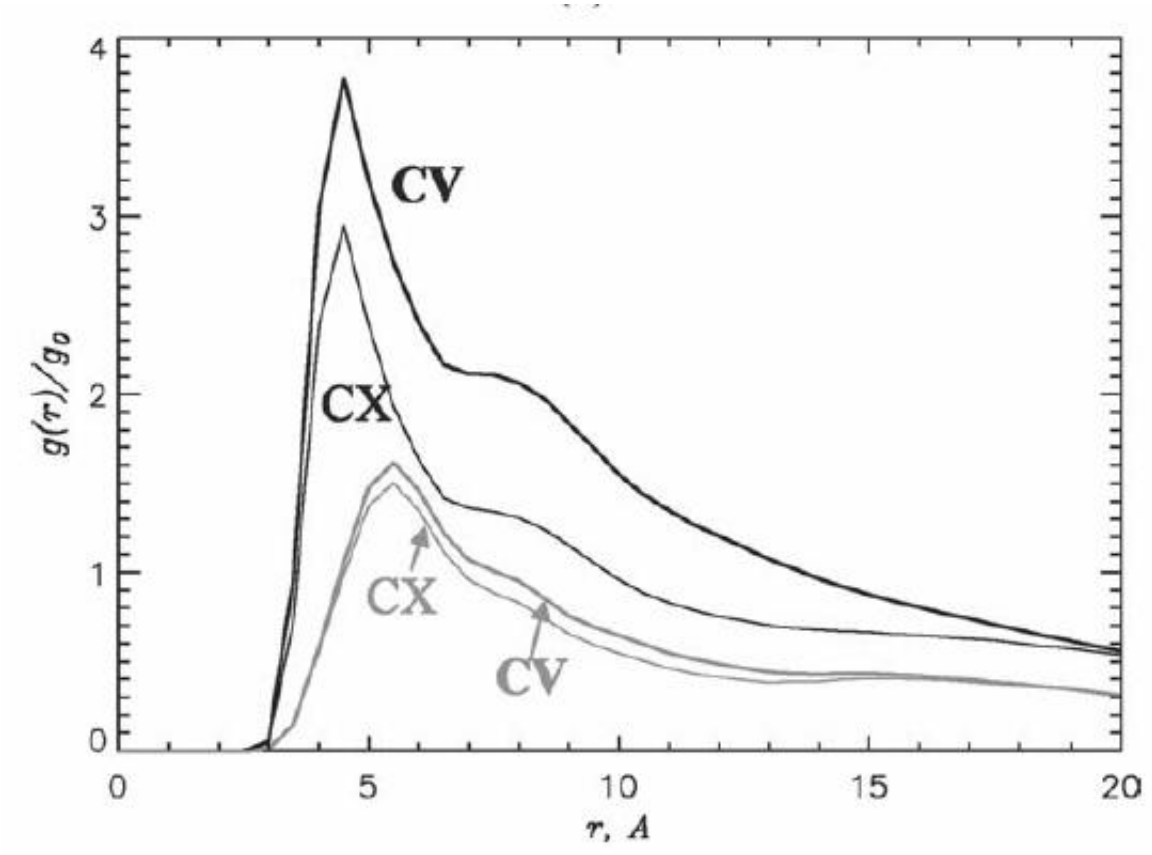

Figure 8 *The radial distribution functions at 360 K for ligand number density, g(r) data*

for naproxen is in black, for ibuprofen - in grey. The distance, r is measured from the ligand center of mass. The functions g(r) are normalized with the bulk value g0.

4.2 DISCUSSION

4.2.1 MECHANISM OF LIGAND BINDING TO ABETA FIBRIL

REMD and atomistic implicit solvent model were used to study the binding of naproxen and ibuprofen to Aβ fibril. For naproxen, it was found that its binding temperature is nearly 40K higher and the binding free energy is 2.4 RT lower than for ibuprofen. It was also found that the distribution of bound naproxen molecules on the fibril surface is highly uneven. For example, naproxen binds more than 2.1 times as often to the CV edge as opposed to the CX edge at 360 K (**Figure 6a**), whereas ibuprofen has nearly the same propensity to bind to the CV compared to the CX edge [13]. However, at 330 K ibuprofen binds 1.5 times as often to the CV edge compared to the CX edge [13]. The inset to **Figure 6a** shows that the binding free energy gap between CV and CX edges is -1.1 RT for naproxen, but is nearly 0 for ibuprofen. This figure also shows that both naproxen and ibuprofen rarely bind to the fibril sides. Thus, naproxen appears to bind with a higher affinity than ibuprofen.

Figure 7 shows that the majority of naproxen ligands cluster in the deep groove of the CV edge and tend to avoid the protrusions of the CX edge. Most (90%) of the ligands form large clusters at the CV edge which suggests cooperative binding (**Figure 7b)**. On the CX edge, only 42% of clusters formed are considered large. At 360 K, the percentage of large clusters formed for ibuprofen on either edge suggests that there is a weak

preference for forming large bound clusters (**Figure 9)**. Furthermore, the radial distribution functions from **Figure 8** indicate that naproxen-naproxen interactions are stronger than those between ibuprofen ligands. Finally, ibuprofen and naproxen have nearly the same numbers of contacts with the fibril. Taken together these observations show the significance of ligand-ligand interactions for binding, so it appears that having more favorable ligand-ligand interactions than ibuprofen is a key factor in naproxen high binding affinity.

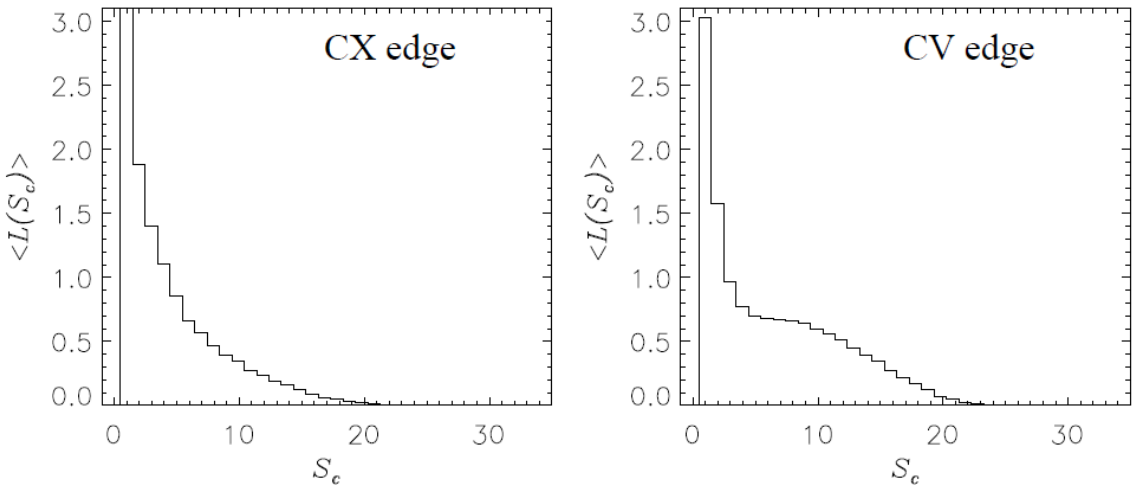

Figure 9 *Distributions of the numbers of bound ibuprofen ligands <L(Sc)> with respect to cluster size Sc on the CX and CV edges.*

To substantiate this conjecture, **Table 1** shows the energetics of naproxen and ibuprofen binding at 360 K. The energies show that ibuprofen forms slightly stronger interactions with the fibril than naproxen does, yet forms considerably weaker (nearly

three-fold) ligand-ligand contacts. Hence, the higher binding affinity of naproxen cannot be due to ligand-fibril contacts, but appears to be due to favorable ligand-ligand contacts. It is possible that the single phenyl ring in ibuprofen forms weaker intermolecular interactions than the naphthalene double rings in naproxen. This conjecture will be revisited below.

Table 1 *Ligand Binding Energetics*

Ligand	**$E_{l\text{-}f}$ (kcal mol^{-1})[a]**	**$E_{l\text{-}l}$ (kcal mol^{-1})[b]**
Naproxen	-7.9	-15.4
Ibuprofen	-8.3	-5.6

[a] *$E_{l\text{-}f}$ is the energy of ligand-fibril interactions. Subscript l=n for naproxen, and l=I for ibuprofen*

[b] *$E_{l\text{-}l}$ is the energy of ligand-ligand interactions.*

The energetics analysis also explains why the binding affinities of the edges (**Table 2**) are different. On the CV edge, the naproxen-fibril contacts are slightly weaker, but the naproxen-naproxen contacts are considerably stronger than on the CX. The potential energy on the CV edge is lower than on the CX edge (a difference of -3.5 kcal mol^{-1}) which suggests that binding to the CV edge is favorable. However, at 360 K, for ibuprofen, the difference between potential energies on the edges is small (-0.3 kcal mol^{-1}), and only becomes considerable (-2.4 kcal mol^{-1}) at 330 K. Hence, the strong interligand interactions induced by confinement of bound ligands to the groove results in the higher affinity of the CV edge.

Table 2 *Energetics of Ligand Binding to the CX and CV Fibril Edges*

	CX		CV	
Ligand	**$E_{l\text{-}f}$ (kcal mol^{-1})[a]**	**$E_{l\text{-}l}$ (kcal mol^{-1})[b]**	**$E_{l\text{-}f}$ (kcal mol^{-1})[a]**	**$E_{l\text{-}l}$ (kcal mol^{-1})[b]**
Naproxen	-9.3	-11.4	-7.3	-16.9
Ibuprofen	-8.6	-5.2	-8.1	-6.0

[a] *$E_{l\text{-}f}$ is the energy of ligand-fibril interactions. Subscript l=n for naproxen, and l=I for ibuprofen*

[b] *$E_{l\text{-}l}$ is the energy of ligand-ligand interactions.*

To further examine the importance of inter-ligand contacts, REMD simulations were performed, in which the non-bonded interactions were switched off between naproxen molecules. This modification resulted in considerable differences in naproxen binding including the reduction in the binding temperature from 398 K to less than 330K. Also, the cancelation of the interligand interactions eliminates naproxen's preference for the CV edge as the numbers of ligands bound to the CV and CX edges for modified naproxen are nearly the same across the entire temperature range (**Figure 10**). In addition, the distributions of bound clusters for modified naproxen become unimodal since the modification blocks the formation of large clusters. These findings lend strong support to the conclusions about the importance of interligand interactions in controlling binding.

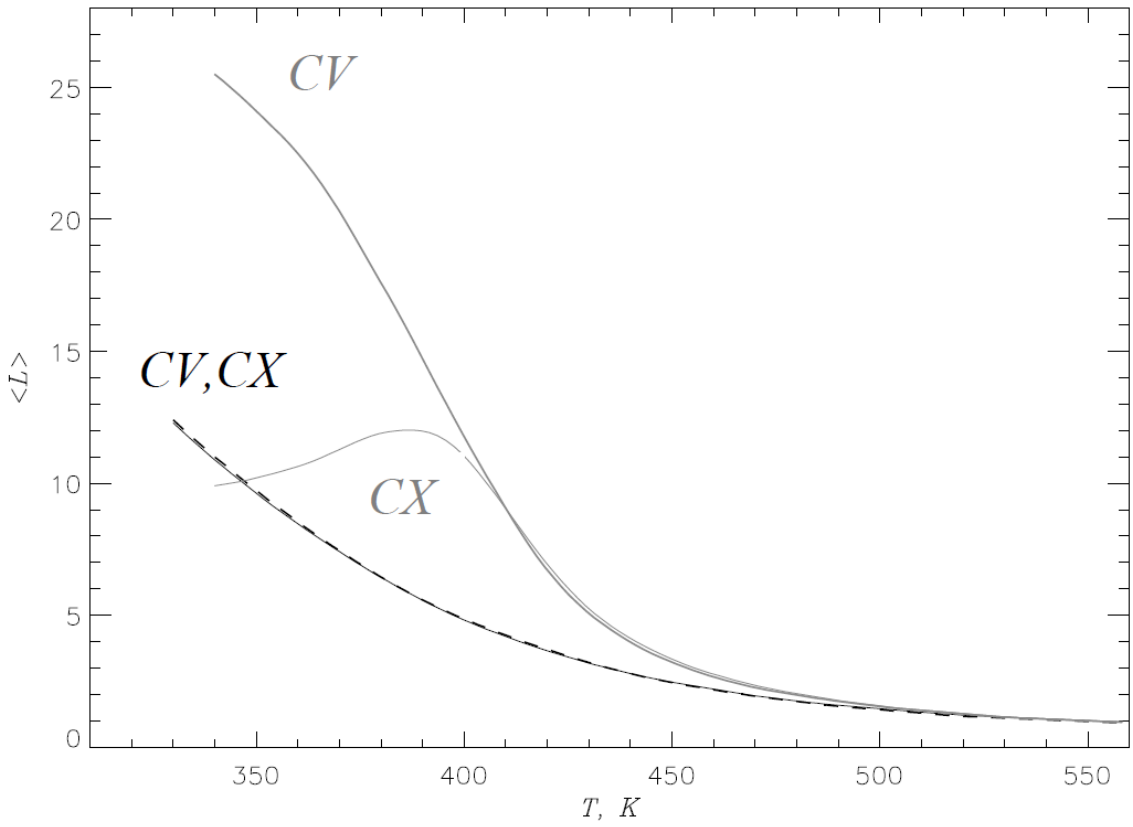

Figure 10 *Binding of "modified" naproxen to the fibril. The quantity <L> represents the numbers of naproxen molecules <L> bound to the CV and CX edges. The data for the naproxen ligands, in which non-bonded interligand interactions are switched off, are shown in black: dashed for CV and thin for CX. The data in grey represent the "original" naproxen simulations (as shown in* ***Figure 6a****): thick line represents CV and thin one is for CX.*

4.2.2 ROLE OF LIGAND CHEMICAL STRUCTURE IN BINDING

More insight as to why ligand-ligand interactions appear important for binding can be gained by evaluating the energetic contributions from different ligand groups: G1, G2, and G3 (**Table 3)**. On the CV edge, the naproxen group G1 contributes -9.9 kcal mol^{-1} (or 59%) to the total interligand energy, G2 (consisting of C1, O2, and C3)

contributes -2.7 kcal mol^{-1} (or 16%), and G3 contributes -5.4 kcal mol^{-1} (or 32%). Similar contributions are obtained for binding to the CX edge. The interactions between these groups are mainly van-der-Waals interactions, with only a minor contribution from electrostatic terms. The analysis is also consistent with the changes in average surface areas (ASAs) of the ligand groups. The average changes in ASA, ΔASA, occurring upon binding to the fibril are ΔASA(G1)=138 $Å^2$, ΔASA(G2)=64 $Å^2$, and ΔASA(G3)=121 $Å^2$, suggesting that G1 buried the most upon binding is the largest contributor to ligand-ligand interaction. For ibuprofen, the interligand interactions contributed by G1, G2, and G3 are -2.2 kcal mol^{-1}, -1.3 kcal mol^{-1}, and -2.5 kcal mol^{-1} respectively, which constitute 37%, 22%, and 42% of the average energy of ligand-ligand interactions on the CV edge. The contributions are similar on the CX edge as was the case with naproxen. For these groups, ΔASA(G1)=61 $Å^2$, ΔASA(G2)=91 $Å^2$, and ΔASA(G3)=95 $Å^2$ due to binding. The energetics and changes in ASA are supportive of the notion that largest contribution to binding is made by the ibuprofen G3 [13]. More significantly, it appears that different structural groups control the binding of naproxen and ibuprofen to the fibril - naphthalene ring G1 for naproxen, and carboxylate G3 group in ibuprofen.

Table 3 *Contributions of Ligand Structural Groups to Binding*

	G1		**G2**		**G3**	
Ligand	**$E_{l\text{-}l}$ (kcal mol^{-1})[a]**	**ΔASA ($Å^2$)[b]**	**$E_{l\text{-}l}$ (kcal mol^{-1})[a]**	**ΔASA ($Å^2$)[b]**	**$E_{l\text{-}l}$ (kcal mol^{-1})[a]**	**ΔASA ($Å^2$)[b]**
Naproxen	-9.9	138	-2.7	64	-5.4	121
Ibuprofen	-2.2	61	-1.3	91	-2.5	95

[a]*$E_{l\text{-}l}$ is the energy of ligand-ligand interactions. Subscript l=n for naproxen and l=i for ibuprofen.*
[b]*ΔASA is the change in accessible surface area upon binding.*

The naphthalene ring's importance in binding has implications for other chemicals with conjugated rings, such as Congo Red (CR) and thioflavin T (ThT) dyes, which are often used for experimental fibril detection. It may be possible that the affinity of CR and ThT to fibrils is at least partly derived from the contacts between conjugated rings in bound ligands.

Our analysis suggests that naproxen and ibuprofen have similar binding mechanisms. Both ligands prefer binding to the CV edge rather than to the CX. Ligand-ligand interactions are induced by the confinement of ligands to the volume of the groove on the CV edge. However, differences in the chemical structure lead to the difference in naproxen and ibuprofen binding. The structure of naproxen enhances its ability to form stronger ligand-ligand interactions compared to ibuprofen, which results in a stronger overall binding affinity.

4.2.3 COMPARISON WITH EXPERIMENTS AND SIMULATIONS

The binding of ibuprofen and naproxen to Aβ fibrils has been previously investigated in the experiments [4, 38]. These ligands share binding sites with the molecular imaging probe ^{18}FFDDNP [38]. Competition curves, which probe the replacement of molecular imaging probe ^{18}FFDDNP with naproxen or ibuprofen, can be used to measure their binding affinities. According to the experiments of Barrio and coworkers [4], half of probe molecules are replaced when the concentration of naproxen

reaches 5.7 nM, but ibuprofen requires concentrations at least twice as large. This observation is consistent with our finding that naproxen binding is noticeably stronger than ibuprofen binding to the Aβ fibril.

Because ^{18}FFDDNP shares binding sites with ibuprofen or naproxen and these three ligands apparently utilize similar binding mechanisms, there are several other considerations worth noting. First, it was reported that only a small number of sites, 3.5 to 7.1 per 10000, were suitable for probe binding [38]. This small number indicates that ligands are bound to only a few places on the fibril surface that seems more consistent with structural features rather than with those of the Aβ sequence. These experimental observations concur with our results implicating the fibril edges as the primary places for binding. Second, the fluorescence data shows that ^{18}FFDDNP probes appear to bind in the hydrophobic clefts on the fibril surface and remain partly hydrated. Localization in the fibril hydrophobic grooves was also observed computationally for ThT dye and its neutral analog BTA-1 [39]. These scenarios concur with our findings that the CV groove rich in hydrophobic amino acids is the primary binding location for naproxen and ibuprofen (**Figure 2a**), while our ASA computations indicate that the bound ligands stay partially exposed to water.

The anti-aggregation effect of naproxen has been studied experimentally [4, 5, 40]. Naproxen was found to limit the accumulation of Aβ fibrils or reduce their ability to grow [5]. The addition of monomers to the edges appears to be the mechanism, which allows amyloid fibrils to grow [41, 42, 43], so the prevention of their extension is consistent with our finding that ligands bind to the fibril edges. The study of Thomas et

al. [40] showed that the coincubation of ibuprofen and naproxen with the fibrils results in a two- and six-fold reduction in the β structure content, respectively. The reduction in the β structure content is higher for naproxen being consistent with that it has higher binding affinity than ibuprofen.

In previous simulations of Aβ fibril elongation, it was shown that incoming Aβ peptides have about 10-fold higher binding affinity for the CV edge as opposed to the CX edge [9, 27]. Our findings indicate that naproxen also prefers to bind to the CV edge and localize within the CV groove, so it is expected to directly compete for the same binding location with incoming Aβ peptides and consequently interfere with the fibril growth. This suggested mechanism of inhibition of fibril growth is supported by experimental results [5] and observations of the similar effects of ibuprofen on Aβ fibril growth.

4.3 CONCLUSIONS

Naproxen and ibuprofen binding to Aβ fibril was examined using REMD and atomistic implicit solvent model. Naproxen's binding temperature is found to be nearly 40 K higher than of ibuprofen, suggesting that naproxen has stronger binding affinity. The crucial contributor to its higher binding affinity is strong interactions between ligands bound to the fibril's surface. The strong interligand interactions appear to be due, in large part, to naproxen's naphthalene rings. Both ligands bind primarily to the concave fibril edge with the groove. Confinement of ligands to the groove is found to facilitate inter-ligand interactions which led to lower energy of ligands bound to the concave edge. Ligand-fibril interactions are similar for both ibuprofen and naproxen and cannot account for the differences in their binding affinity. Our simulations provide a rationale for

different binding affinities of naproxen and ibuprofen observed experimentally.

5. IMPACT OF IBUPROFEN ON Aβ FIBRIL GROWTH

5.1 RESULTS

5.1.1 IBUPROFEN SUPPRESSES ASSOCIATION OF AB PEPTIDES WITH THE FIBRIL

To understand the association of incoming Aβ peptides with the fibril, the number of parallel hydrogen bonds (N_{phb}), the number of hydrogen bonds (N_{hb}), and the number of hydrophobic contacts (C_h) were determined between incoming Aβ peptides and the fibril in ibuprofen aqueous solution at the temperatures 330 K through 600 K (System 2, **Figure 11**). The results indicate that the peptide-fibril interactions increase as the temperature decreases. More importantly, this figure indicates that the peptide-fibril binding affinity tends to be higher in water as compared to the ibuprofen solution. Similar conclusion follows from **Table 4**, which lists different forms of peptide-fibril interactions. At the temperature 360K corresponding to locking transition of incoming Aβ peptide in water [13], there is a 20-30% reduction in the overall peptide-fibril interactions in the ibuprofen solution compared to water. This suggests that ibuprofen can potentially destabilize binding of Aβ peptides to the fibril.

Table 4 *The number of different interactions formed between incoming Aβ peptide and the fibril at 360 K. C_h, N_{hb}, and N_{phb} represent the number of hydrophobic contacts, the number of hydrogen bonds, and the number of parallel hydrogen bonds, respectively.*

Solution	**C_h**	**N_{hb}**	**N_{phb}**
Water	9.8	10.5	6.0
Ibuprofen	7.1	8.0	4.7

Table 5 *Free energy of binding of ibuprofen to Aβ species at 360K*

Abeta species	Fibril	Fibril + incoming peptides
$\Delta F_b/RT$	-5.6	-5.6

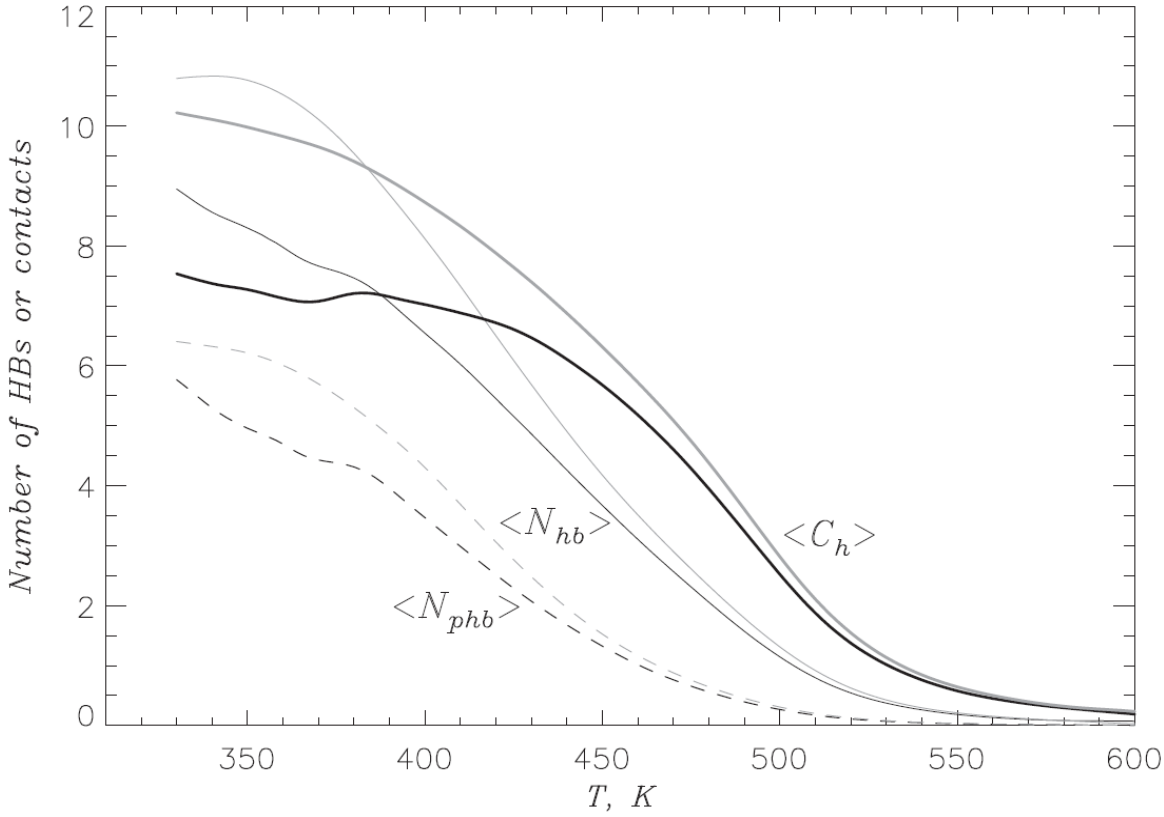

Figure 11 *Binding of Aβ10–40 peptides to the fibril is described by the thermal averages of hydrophobic contacts <$C_h(T)$> (thick lines), the number of HBs <$N_{hb}(T)$> (thin lines), and the number of parallel HBs <$N_{phb}(T)$> (dashed lines). The data in solid and grey are obtained in ibuprofen solution and water, respectively. The plot indicates that ibuprofen suppresses Aβ binding to the fibril.*

5.1.2 IBUPROFEN BINDS TO AB SPECIES

To understand how ibuprofen impacts Aβ fibril growth, the free energy of binding (F_b) was studied for ibuprofen while interacting with Aβ hexameric system (i.e., System 2). The free energy profile was measured as a function of distance between a ligand and the surface of hexamer at 360 K (**Figure 12**). The probabilities of ibuprofen

binding to the hexamer as a function of temperature were also determined. As shown in the inset in **Figure 12**, the binding midpoint occurs around 376 K. At 360 K, the probability of binding (P_b) for ibuprofen is 0.63 and the number of bound ligands is 38.0 (out of 60). The probability for ibuprofen binding simultaneously to the fibril and incoming peptides P_{bi} is 0.2 and the number of such bound ligands is 11.7. This observation implies that about 30% of bound ligands are localized at the peptide-fibril interface.

From **Figure 12** the binding free energy can be obtained using Eq. 1 above. The result shows that $\Delta F_b \approx$ -5.6 RT for binding of ibuprofen to the Aβ hexamer (**Table 5**). In the previous work [13], ΔF_b was measured to be around -5.6 RT for the binding of ibuprofen to the fibril alone (without incoming peptides, i.e., System 1). This suggests that thermodynamic binding preference for ibuprofen is not significantly affected by incoming peptides. More importantly, the free energy computations implicate strong binding affinity of ibuprofen that may lead to the destabilization of peptide-fibril interactions.

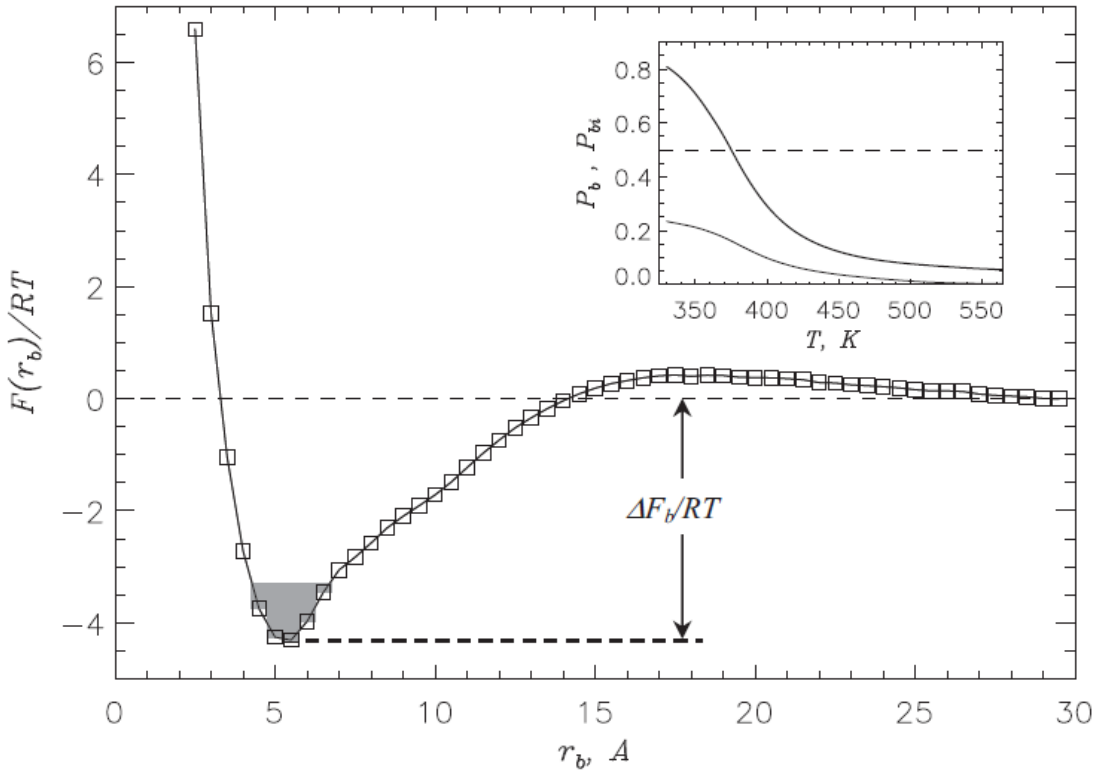

Figure 12 *Free energy of ibuprofen binding to Aβ hexamer as a function of the distance between ibuprofen and Aβ surface at 360 K. All values of F at r_b>29 Å are set to zero. (Inset) Probabilities of ibuprofen binding to Aβ (thick line) and to aggregation interface (thin line) as a function of temperature.*

5.1.3 IMPACT OF IBUPROFEN ON FIBRIL ELONGATION

To see whether ibuprofen can impact Aβ fibril growth, the free energy landscapes F(C) describing peptide-fibril interactions in water and ibuprofen environments were computed. Here, C is the number of side chain peptide-fibril contacts. As shown in **Figure 13a**, both free energy profiles feature a single minimum.

This observation is consistent with the barrierless nature of binding of Aβ peptides to the fibril [9]. The number of side chain contacts C at the energy minimum is smaller for the ibuprofen environment than for water.

The difference in the free energies of bound and unbound peptide states ΔF_{B-U} can be determined using Eq. (1) (**Table 6**). These computations reveal an increase of 2.5 RT in the free energy for peptide-fibril binding in ibuprofen solution in contrast to the binding in water (**Figure 13a and Table 6**). However, compared to the binding free energy of ibuprofen (ΔF_b=-5.6RT) the free energy gain of Aβ binding to the fibril in ibuprofen environment ($\Delta F_{B-U} \approx$ -7.4 RT) is still sufficient to result in peptide docking (**Fig. 2b**).

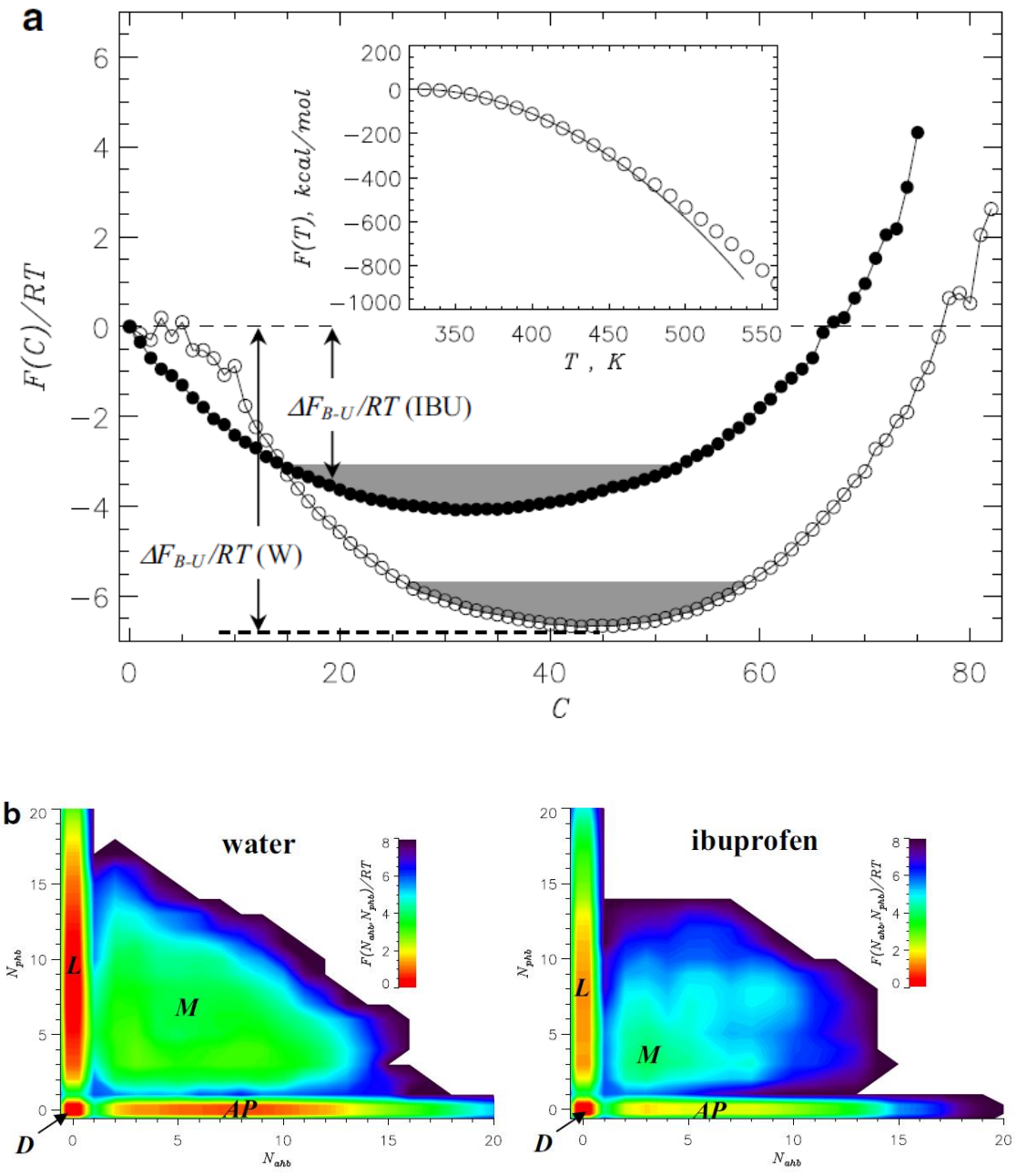

Figure 13 (a) *Free energy of incoming Aβ peptide F(C) as a function of the number of peptide-fibril side-chain contacts C in water (open circles, W) and in ibuprofen solution (solid circles, IBU). The free energy of Aβ binding to the fibril is* $\Delta F_{B-U} = F_B - F_U$*, where* F_B *and* $F_U = 0$ *are the free energies of bound (B) and unbound (U, C = 0) states.* F_B *is computed by integrating over the B states (shaded) with* $F(C) \leq F_{min} + 1.0$ *RT, where* F_{min} *is the minimum in F(C). The plot shows that ibuprofen destabilizes Aβ binding to the fibril.* ***(Inset)*** *Temperature dependence of the system free energy F(T)*

calculated self-consistently from the multiple histogram method [35]. Quadratic fitting function, from which the docking temperature T_d is estimated, is shown by the solid continuous curve. Maximum value of F(T) is set to zero. ***(b)*** *Free energy surfaces $F(N_{ahb}, N_{phb})$ for bound Aβ peptide as a function of the number of antiparallel HBs N_{ahb} and parallel HBs N_{phb} formed between the peptide and the fibril. The locked (L), antiparallel (AP), docked (D), and mixed (M) states are marked. The free energy landscapes show that, due to ibuprofen, the L state becomes less stable with respect to state D. Panels a and b are computed at 360 K.*

Table 6 *Binding of incoming Aβ peptides to amyloid fibril at 360K. ΔF_{B-U} is the difference in free energies between the bound and unbound states. ΔF_{L-D} is the free energy difference between the locked and docked states. $\Delta F'$ represents the free energy escape barrier for the locked state.*

Environment	$\Delta F_{B-U}/RT$	$\Delta F_{L-D}/RT$	$\Delta F'/RT$
Water	-9.9	-2.0	3.8
Ibuprofen	-7.4	-1.0	2.8

Assuming that docking is a continuous transition, the docking temperature T_d can be estimated from the temperature dependence of the system free energy F(T). To this end, the quadratic fitting equation $F(T) = -\alpha(T-T_d)$, where α is a constant, were utilized [9]. As shown in the inset to **Figure 12**, a good fit to F(T) is obtained at $T \leq 450$ K, when $\alpha = 0.019$kcal/(mol K^2), and $T_d = 322$ K. In comparison, in water T_d is estimated to be 380 K. The result suggests that ibuprofen binding reduces the docking temperature by approximately 60 K.

To quantify the effect of ibuprofen on the locking transition, the free energy landscape $F(N_{phb},N_{ahb})$ was examined, where N_{phb} is the number of parallel hydrogen

bonds and N_{ahb} is the number of anti-parallel hydrogen bonds (**Figure 13b**). (A peptide-fibril parallel hydrogen bond is formed between the residues i and j, if at least one other hydrogen bond is present between residues i+2 and j or j+2 or between i-2 and j or j-2. A peptide-fibril antiparallel hydrogen bond is formed between the residues i and j, if at least one other hydrogen bond is also formed between residues i-2 and j+2 or between i+2 and j-2.) These quantities are designed to measure the amount of parallel and antiparallel β-sheets. The following free energy basins in **Figure 13b** associated with different β-sheet conformations can be distinguished: Mixed (M) with $N_{phb}>3$ and $N_{ahb}>3$, antiparallel (AP) with $N_{phb}=0$ and $N_{ahb}>3$, locked (L) with $N_{phb}>3$ and $N_{ahb}=0$, and docked (D) with $N_{phb}=0$ and $N_{ahb}=0$ [9]. In **Figure 13b** the differences in the equilibrium distributions of peptide bound states in two environments are clearly visible. In ibuprofen solution L, AP, and M states become less stable compared to the D state. The free energy gap between L and D is reduced by approximately 1.0 RT in the ibuprofen solution (**Table 6**). The locking temperature T_l is defined to be the temperature, at which the population of the L state is 0.5. Using this definition T_l is 330K in ibuprofen solution compared to $T_l \approx 360$K in water [9]. Therefore, ibuprofen lowers the locking temperature by 30K. Additionally, the escape barrier between L and D states is lowered (**Table 6**). Hence ibuprofen destabilizes Aβ locked state relative to disordered docked states.

5.2 DISCUSSION

5.2.1 FREE ENERGY LANDSCAPE OF FIBRIL GROWTH IN IBUPROFEN SOLUTION

Ibuprofen was demonstrated to weaken the interactions between incoming peptides and the fibril. According to **Table 6**, ibuprofen reduces the free energy gain for peptide binding implying that the bound state of Aβ peptides becomes less stable in ibuprofen solution than in water. Further, the free energy difference that separates the locked and docked states is smaller for ibuprofen than for water. The peptide-fibril interactions such as hydrogen bonding and side chain contacts are reduced by 20-40% when ibuprofen is present in solution (**Figure 11**). The temperatures for docking and locking transitions are lower by 60K and 30K in ibuprofen solution compared to those in water, respectively. However, by comparing the free energy of ibuprofen binding to the fibril ΔF_b at 360K (**Table 5**) with the free energy of Aβ binding $\Delta F_{B\text{-}U}$ in **Table 6** one can conclude that ΔF_b is at least 4.3 RT higher than $\Delta F_{B\text{-}U}$. Therefore, Aβ peptides have still stronger binding affinity to Aβ fibril than ibuprofen does. Although ibuprofen reduces the free energy gain for peptide binding (**Table 6**) and destabilizes peptide-fibril interaction, it fails to completely block Aβ fibril growth.

5.2.2 MOLECULAR BASIS OF IBUPROFEN ANTI-AGGREGATION EFFECT

Previous studies have computed the number of ibuprofen ligands bound to the concave (CV) and convex (CX) edges [13]. The binding (CV:CX) ratios are 2:1 at 330K and 1.4:1 at 360K. The result indicates that ibuprofen tends to bind to the concave (CV) edge of the fibril, which interestingly is also the primary binding site for the incoming peptides [9].

Therefore, ibuprofen competes with incoming peptides for the same binding site on Aβ fibril. It is conceivable that the second factor also contributes to anti-aggregation effect. The free energy was computed for binding of incoming peptides to CV and CX edges in water and ibuprofen solutions. In ibuprofen solution, the free energy difference between the CV and CX bound states $\Delta F_{CV\text{-}CX} \approx 1.5$ RT, whereas in water, $\Delta F_{CV\text{-}CX} \approx 2.5$ RT. The finding implies that a fraction of Aβ peptides is forced to bind to the low affinity CX edge instead of high affinity CV one.

To determine the energetic factors affecting ibuprofen binding to the fibril, the average intermolecular energy E_{inter} and the average solvation energy E_{solv} per ibuprofen molecule were computed at 360K. The change of E_{inter} between bound and unbound states is -12.5kcal/mol (unbound: -1.4 kcal/mol; bound: -13.9 kcal/mol), while the difference in E_{solv} is 1.0kcal/mol. The van der Waals (vdW) interactions appear to be the key contribution to $\Delta E_{inter,}$ since they make up more than 90% of the energy value. Therefore, vdW interaction is the major factor involved in ibuprofen binding. The finding was further supported by computing the change of accessible surface area (ASA) in bound and unbound states at 360K. The average ASAs for the three groups G1, G2, and G3 (**Figure 3**) in unbound ibuprofen are 90 $Å^2$, 161 $Å^2$, and 153 $Å^2$, respectively. For bound ibuprofens, the average ASAs for G1, G2, and G3 are 37 $Å^2$, 83 $Å^2$, and 68 $Å^2$, respectively. Due to significant changes in ASAs for G2 (78 $Å^2$) and G3 (85 $Å^2$), it appears that G2 and G3 are the key groups for ibuprofen binding to the fibrils. The limited role of G1 in binding could be due to the fact that its aromatic ring is inflexible. Also, G1 is sandwiched between the G2 and G3 groups that should impede its

interactions with the fibril. The ASA computations are consistent with the vdW observations in that ibuprofen binding mainly involves hydrophilic G3 group (**Figure 3 - Section 3.4**). This finding is also consistent with previous results suggesting that ibuprofen binding sites include a mixture of hydrophobic and hydrophilic residues [13].

5.2.3 EXPERIMENTAL EVIDENCE

Previous experimental results have demonstrated anti-aggregate effect of ibuprofen with respect to Aβ fibrils elongation. McKee et al has shown that ibuprofen reduces the amount of Aβ oligomers in mice brain tissues [44]. Yamada's group has demonstrated that ibuprofen can inhibit fibril elongation while incubating Aβ peptides in high concentration of ibuprofen (at the ratio of ibuprofen to fibril peptides of 22:1) [5]. However, the exact extent of blocking fibril growth is concentration dependent. These experimental observations are consistent with the simulation outcomes that ibuprofen destabilizes the interactions of peptides with Aβ fibril and that ibuprofen impedes but does not block fibril elongation.

5.3 CONCLUSIONS

The in silico results revealed that ibuprofen interferes with the binding of Aβ peptides to the amyloid fibril. In particular, ibuprofen reduces the free energy gain of peptide binding to the fibril. Furthermore, ibuprofen interactions shift the thermodynamic equilibrium from fibril-like locked peptide state to disordered docked state. From molecular perspective, anti-aggregation effect of ibuprofen is based on direct competition between Aβ peptides and ligands for binding to the same Aβ fibril location (the CV edge of the fibril).

6. BINDING OF NAPROXEN TO Aβ MONOMER

6.1 APPLICATION OF AUTODOCK TO PROBE NAPROXEN BINDING

To study binding of naproxen to Aβ monomer, the software package AutoDock 4.2 was utilized. As described in Methods the ensembles of Aβ conformations generated by REMD were employed as protein structures to initiate ligand docking simulations. It is important to note that AutoDock uses a semiempirical force field derived from the analysis of structures and inhibition constants for known protein-ligand complexes. To examine robustness of docking results, the docking simulations were performed using simulated annealing (SA) and Lamarckian genetic algorithm (LGA) and compared. According to **Figure 14** similar binding probabilities $P_b(i)$ for Aβ residues were obtained using both of these methods. Consequently, all subsequent AutoDock simulations were performed using the LGA method. **Figure 14** also shows that naproxen preferably binds to the N-terminal region of the Aβ monomer.

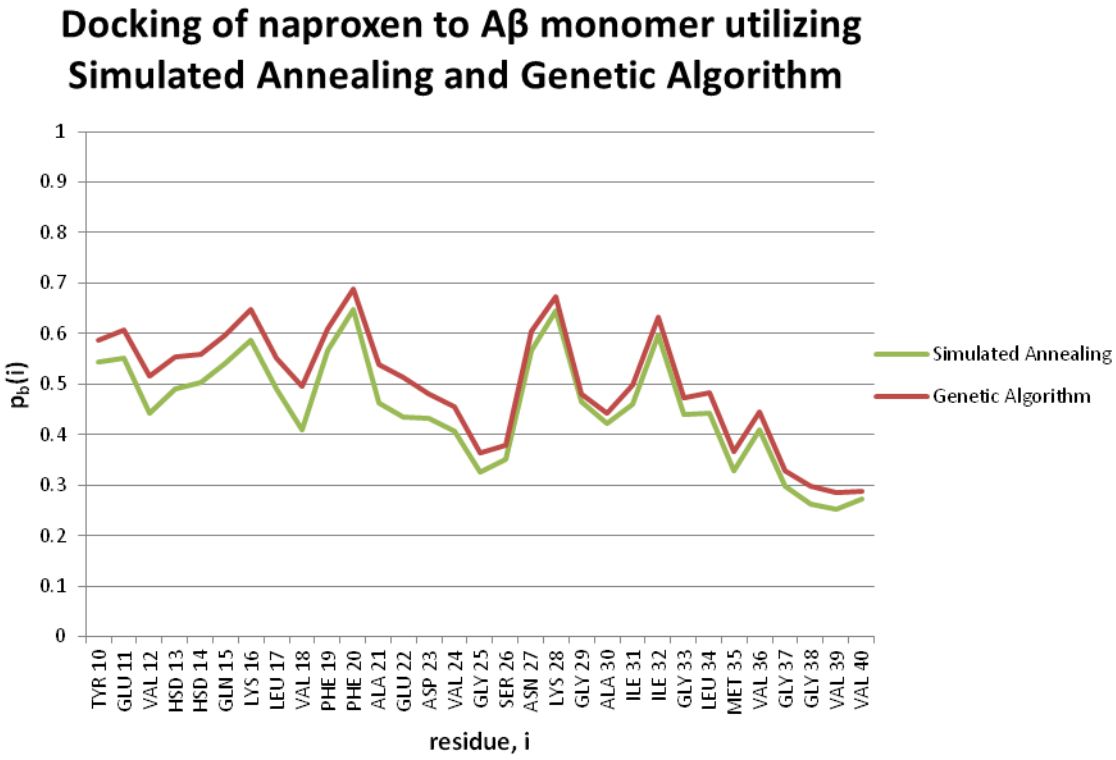

Figure 14 *Probability $P_b(i)$ of naproxen binding to amino acids i in Aβ monomer. The results of binding Autodock simulations were tested by applying SA and LGA algorithms. The figure reveals almost identical $P_b(i)$ profiles for both algorithms.*

The AutoDock binding probabilities were further compared with the implicit solvent REMD results obtained for Aβ dimer coincubated with 20 naproxen molecules [12]. Because the AutoDock docking simulations can only occur at 298K, the REMD data was computed at the lower temperature of 330K, which is closer to physiological regime than 360K (note that naproxen binding propensities at 330K and 360K are qualitatively similar). For REMD simulations, in lieu of binding probabilities the numbers of contacts formed by amino acids i with the ligands, $<C_l(i)>$ were used. As

shown in **Figure 15**, the propensities of binding to Aβ residues are quite similar between AutoDock and the implicit solvent REMD methods. For example, the correlation factor computed between $P_b(i)$ and $<C_l(i)>$ is 0.66. This comparison offers stringent test of naproxen binding mechanism, because it involves two independent force fields and two different Aβ species, monomer and dimer.

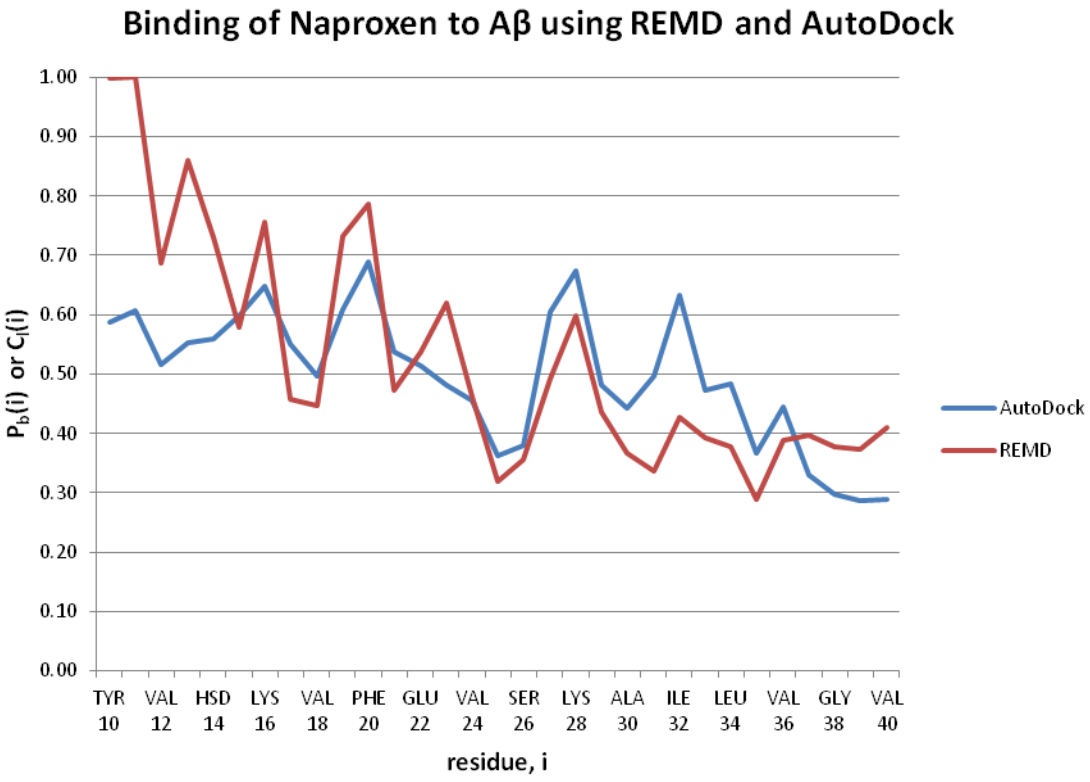

Figure 15 *Probabilities $P_b(i)$ of naproxen binding to Aβ monomer computed using AutoDock are compared with the numbers of contacts formed by amino acids with the ligands $<C_l(i)>$ obtained from REMD simulations. Amino acid index is denoted as i. The results indicate that naproxen binds preferentially to the N-terminal region of Aβ peptide.*

To determine the factor which controls naproxen preferential binding to the N-terminal, AutoDock simulations were performed for the mutant $A\beta_{10\text{-}40}$ monomer, in which the order of amino acids in the sequence was reversed. To this end, the same ensemble of monomer structures employed for studying binding to the wild-type Aβ monomer was used. The reversed Aβ sequence was then "fitted" into each structure in the ensemble. **Figure 16** compares the probabilities of binding $P_b(i)$ to amino acids in both sequences. When the data for the reversed sequence are arranged in backward direction, the correlation coefficient between the wildtype and the mutant $P_b(i)$ reaches 0.91. **Figure 16** also allows us to identify the set of amino acids with high affinity of binding naproxen. The list of ten high affinity amino acids includes PHE, LYS, GLN, and ASN. In particular, two PHE (at positions 19 and 20), one GLN (at position 15), two LYS (at positions 16 and 28), and one ASN (at 27) generally appear in the N-terminal region (residues 10 through 23). Comparison of the binding probabilities for the wild-type and reversed sequences gives a compelling argument that the binding of naproxen to Aβ monomer is driven by the interactions with amino acids.

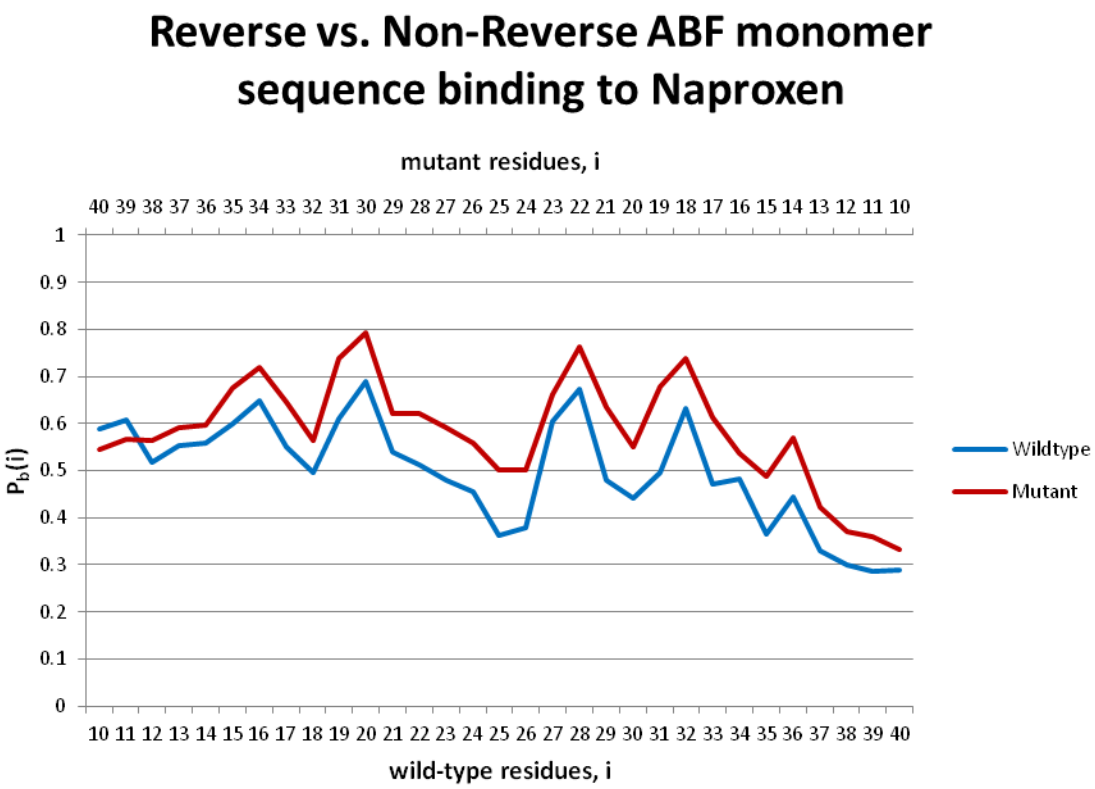

Figure 16 *Probabilities of naproxen binding to Aβ monomers with reversed and non-reversed (wild-type) sequences, $P_b(i)$. The probability distribution for the reversed sequence is plotted backward to facilitate comparison of binding patterns.*

6.2 DISCUSSION

AutoDock simulations do not consider ligand-ligand interactions. In contrast, REMD simulations probing binding of naproxen to Aβ dimer incorporate interligand interactions [12]. Nevertheless, similar binding results have emerged from both applications indicating that the elimination of the inter-ligand interactions by Autodock does not alter the binding physics. The results presented in this section suggest that the

binding mechanisms for Aβ fibrils and monomers are fundamentally different. In case of fibril binding, NSAID ligands tend to bind to the groove on the CV edge and their binding mechanism is mainly driven by the fibril surface geometry and interligand interactions (described in Sections 4.1.1 and 4.1.2). In case of binding to Aβ monomers, ligand interactions with amino acids appear to control binding (described in Section 6.1.1). This conclusion is strongly supported by the close similarity in the distributions of binding locations for the wild-type and reversed Aβ sequences (**Figure 16**). It is likely that the lack of stable structure in Aβ monomers prevents the formation of grooves similar to those observed in amyloid fibrils that in turn eliminates surface geometry as a binding factor.

6.3 CONCLUSION

This study demonstrates that the results obtained from the implicit solvent REMD and AutoDock simulations are consistent in identifying binding locations of naproxen in Aβ monomer. More importantly, the result shows that the mechanisms of ligand binding to Aβ monomers and fibrils are fundamentally different. Binding to amyloid fibrils is mainly controlled by the fibril surface geometry and interligand interactions, whereas binding to Aβ monomer is governed by peptide sequence. Finally, this difference can be exploited in the future in the design of molecular markers or therapeutic agents, which selectively recognize particular Aβ species.

REFERENCES

REFERENCES

[1] Brookmeyer R, Johnson E, Ziegler-Graham K, Arrighi MH. (2007). "Forecasting the global burden of Alzheimer's disease". Alzheimer's and Dementia. 3(3): 186–91.

[2] George AR, Howlett DR. (1999). Computationally Derived Structural Models of the b-Amyloid Found in Alzheimer's Disease Plaques and the Interaction with Possible Aggregation Inhibitors. Bioplymers. 50, 733-741.

[3] Arispe N, Diaz JC, Simakova O. (2007). Abeta ion channels. prospects for treating alzheimer'sdisease with abeta channel blockers. Biochim. Biophys. Acta, **1768**, 1952–1965.

[4] Agdeppa ED, Kepe V, Petric A, Satyamurthy N, Liu J, Huang SC, Small GW, Cole GM, Barrio JR. (2003). In vitro detection of (s)-naproxen and ibuprofen binding to plaques in the Alzheimer's brain using the positron emission tomography molecular imaging probe 2-(1-{6-[(2-[18F]fluoroethyl)(methyl)amino]-2-naphthyl}ethylidene) malononitrile. Neurosci. 117, 723–730.

[5] Hirohata M, Ono K, Naiki H, Yamada M. (2005). Non-steroidal anti-inflammatory drugs have anti-amyloidogenic effects for Alzheimer's β-amyloid fibrils in vitro. Neuropharmacology. 49, 1088-1099.

[6] Pavani P, Mangala SD, Murthy JVVS, Babu AP. (2008). Protein-Ligand Interaction Studies on 2,4,6-trisubstituted triazine derivatives as anti-malarial DHFR agents using AutoDock. Res. J. Biotechnol. 3, 18.

[7] Perola EW, Walters P, Charifson PS. (2004). A detailed comparison of current docking and scoring methods on systems of pharmaceutical relevance. Proteins. 56, 235-249.

[8] Takeda T, Klimov DK. (2009). Probing the effect of amino-terminal truncation for Abeta1-40 peptides. J. Phys. Chem. B. 113, 6692-6702.

[9] Takeda T, Klimov DK. (2009). Replica exchange simulations of the thermodynamics of Abeta fibril growth. Biophysical J. 96, 442-452.

[10] Chang WE, Takeda T, Raman EP, Klimov DK. (2010). Molecular dynamics simulations of anti-aggregation effect of ibuprofen. Biophysical J. 98, 2662–2670.

[11] Takeda T, Chang WE, Raman EP, Klimov DK. (2010). Binding of non-steroidal anti-inflammatory drugs to Aβ fibril. Proteins Struct. Funct. Bioinform. 78, 2859-2860.

[12] Kim S, Chang WE, Kumar R, Klimov DK. (2011). Naproxen interferes with the assembly of Abeta oligomers implicated in Alzheimer's disease. Biophys. J. (accepted).

[13] Raman EP, Takeda T, Klimov DK. (2009). Molecular dynamics simulations of ibuprofen binding to Aβ peptides. Biophysical J. 97, 2070–2079.

[14] Paravastu AK, Petkova AT, Tycko R. (2006) Polymorphic fibril formation by residues 10–40 of the Alzheimer's beta-amyloid peptide. Biophysical J 90, 4618–4629.

[15] Petkova AT, Yau WM, Tycko R. (2006). Experimental constraints on quaternary structure in Alzheimer's beta-amyloid fibrils. Biochemistry. 45, 498-512.

[16] Petkova AT, Ishii Y, Balbach JJ, Antzutkin ON, Leapman RD, Delaglio F, Tycko R. (2002). A structural model for Alzheimer's β-amyloid fibrils based on experimental constraints from solid state NMR. Proc. Natl. Acad. Sci. 99, 16742–16747.

[17] Tycko R. (2006). Molecular structure of amyloid fibrils: Insights from solid state NMR. Q. Rev. Biophys. 39, 1-55.

[18] Brooks BR, Bruccoler RE, Olafson BD, States DJ, Swaminathan S, Karplus M. (1982) CHARMM: a program for macromolecular energy, minimization, and dynamics calculations. J Comp Chem. 4, 187–217.

[19] Ferrara P, Apostolakis J, Caflisch A. (2002). Evaluation of a fast implicit solvent model for molecular dynamics simulations. Proteins. 46, 24–33.

[20] Takeda T, Klimov DK. (2009). Interpeptide interactions induce helix to strand structural transition in Aβ peptides. Proteins Struct. Funct. Bioinform. 77, 1–13.

[21] Hou L, Shao H, Zagorski MG. (2004). Solution NMR studies of the Aβ(1–40) and Aβ(1–42) peptides establish that the Met35 oxidation state affects the mechanism of amyloid formation. J. Am. Chem. Soc. 126, 1992–2005.

[22] Fleischman SH, Brooks CL. (1990). Protein-Drug interactions: Characterization of inhibitor binding in complexes of DHFR with trimethoprim and related derivatives. Proteins Struct. Funct. Bioinform. 7, 52-61.

[23] Antzutkin ON, Leapman RD, Balbach JJ, Tycko R. (2002). Supramolecular structural constraints on Alzheimers β-amyloid fibrils from electron microscopy and solid-state nuclear magnetic resonance. Biochemistry. 41, 15436–15450.

[24] Zhou Y, Vitkup D, Karplus M. (1999). Native proteins are surfacemolten solids: application of the Lindemann criterion for the solid versus liquid state. J. Mol. Biol. 285, 1371–1375.

[25] Meersman F, Dobson CM. (2006). Probing the pressure-temperature stability of amyloid fibrils provides new insights into their molecular properties. Biochim. Biophys. Acta. 1764, 452–460.

[26] Sugita Y, Okamoto Y. (1999). Replica-exchange molecular dynamics method for protein folding. Chem. Phys. Lett. 114, 141–151.

[27] Takeda T, Klimov DK. (2009). Probing energetics of abeta fibril elongation by molecular dynamics simulations. Biophysical J. 96, 4428–4437.

[28] Garcia AE, Onuchic JN. (2003). Folding a protein in a computer: an atomic description of the folding/unfolding of protein A. Proc. Natl. Acad. Sci. USA. 100, 13898–13903.

[29] Cecchini M, Rao F, Seeber M, Caflisch A. (2004). Replica exchange molecular dynamics simulations of amyloid peptide aggregation. J. Chem. Phys. 121, 10748–10756.

[30] Baumketner A, Shea JE. (2007). The structure of Alzheimer amyloid b 10–35 peptide probed through replica exchange molecular dynamics simulations in explicit solvent. J. Mol. Biol. 366, 275–285.

[31] Jang S, Shin S. (2008). Computational study on the structural diversity of amyloid beta-peptide (Ab10–35) oligomers. J. Phys. Chem. B. 112, 3479–3484.

[32] Tsai HH, Reches M, Tsai CJ, Gunasekaran K, Gazit E, Nussinov R. (2005). Proc. Natl. Acad. Sci. USA. 102, 8174–8179.

[33] Kabsch W, Sander C. (1983). Dictionary of protein secondary structure: pattern recognition of hydrogen-bonded and geometrical features. Biopolymers 22, 2577–2637.

[34] Lee B, Richards FM. (1971). The interpretation of protein structures: estimation of static accessibility. J Mol Biol. 55, 379–400.

[35] Ferrenberg AM, Swendsen RH. (1989). Optimized Monte Carlo data analysis. Phys. Rev. Lett. 63, 1195–1198.

[36] Takeda T, Kumar R, Raman EP, Klimov DK. (2010). Non-steroidal anti-inflammatory drug naproxen destabilizes Abeta amyloid fibrils: A molecular dynamics investigation J. Phys. Chem. B 114, 15394-15402.

[37] Moris GM, Huey R, Lindstrom W, Sanner MF, Belew RK, Goodsell DS, Olson AJ. (2009). AutoDock4 and AutoDockTools4: Automative docking with selective receptor exibility. J. Comp. Chem. 30, 2785-2791.

[38] Agdeppa E, Kepe V, Liu J, Flores-Torres S, Satyamurthy N, Petric A, Cole GM, Small GW, Huang S-C, Barrio JR. (2001). Binding characteristics of radiofluorinated 6-dialkylamino-2-naphthylethylidene derivatives as positron emission tomography imaging probes for b-amyloid plaques in Alzheimers disease. J Neurosci. 21, 1–5.

[39] Wu C, Wang Z, Lei H, Duan Y, Bowers MT, Shea J-E. (2008). The binding of thioflavin T and its neutral analog BTA-1 to protofibrils of the Alzheimer's disease a b16–22 peptide probed by molecular dynamics simulations. J Mol Biol. 384, 718–729.

[40] Thomas T, Nadackal TG, Thomas K. (2001). Aspirin and non-steroidal anti-inflammatory drugs inhibit amyloid- baggregation. NeuroReport. 12, 3263–3267.

[41] Esler WP, Stimson ER, Jennings JM, Vinters HV, Ghilardi JR, Lee JP, Mantyh PW, Maggio JE. (2000). Alzheimer's disease amyloid propagation by a template-dependent dock-lock mechanism. Biochemistry. 39, 6288–6295.

[42] Cannon MJ, Williams AD, Wetzel R, Myszka DG. (2004). Kinetic analysis of beta-amyloid fibril elongation. Anal Biochem. 328, 67–75.

[43] Ban T, Hoshino M, Takahashi S, Hamada D, Hasegawa K, Naiki H, Goto Y. (2004). Direct observation of Aβ amyloid fibril growth and inhibition. J Mol Biol. 344, 757–767.

[44] McKee AC, Carreras I, Dedeoglu A. (2008). Ibuprofen reduces Aβ, hyperphosphorylated tau and memory deficits in Alzheimer mice. Brain Res. 1207, 225–236.

CURRICULUM VITAE

Wenling E. Chang received her Bachelor of Science from University of Maryland Baltimore County in 2001. She was employed at Walter Reed Army Institute of Research for one year and received her Master of Science from Johns Hopkins University in 2004. She has been employed at the MITRE Corporation since 2004.